

## Geological Society of America Bulletin

### Kinematic evolution of the Patagonian retroarc fold-and-thrust belt and Magallanes foreland basin, Chile and Argentina, 51°30 'S

Julie C. Fosdick, Brian W. Romans, Andrea Fildani, Anne Bernhardt, Mauricio Calderón and Stephan A. Graham

*Geological Society of America Bulletin* 2011;123;1679-1698  
doi: 10.1130/B30242.1

---

- Email alerting services** click [www.gsapubs.org/cgi/alerts](http://www.gsapubs.org/cgi/alerts) to receive free e-mail alerts when new articles cite this article
- Subscribe** click [www.gsapubs.org/subscriptions/](http://www.gsapubs.org/subscriptions/) to subscribe to Geological Society of America Bulletin
- Permission request** click <http://www.geosociety.org/pubs/copyrt.htm#gsa> to contact GSA

Copyright not claimed on content prepared wholly by U.S. government employees within scope of their employment. Individual scientists are hereby granted permission, without fees or further requests to GSA, to use a single figure, a single table, and/or a brief paragraph of text in subsequent works and to make unlimited copies of items in GSA's journals for noncommercial use in classrooms to further education and science. This file may not be posted to any Web site, but authors may post the abstracts only of their articles on their own or their organization's Web site providing the posting includes a reference to the article's full citation. GSA provides this and other forums for the presentation of diverse opinions and positions by scientists worldwide, regardless of their race, citizenship, gender, religion, or political viewpoint. Opinions presented in this publication do not reflect official positions of the Society.

---

#### Notes

# Kinematic evolution of the Patagonian retroarc fold-and-thrust belt and Magallanes foreland basin, Chile and Argentina, 51°30'S

Julie C. Fosdick<sup>1,†</sup>, Brian W. Romans<sup>2</sup>, Andrea Fildani<sup>2</sup>, Anne Bernhardt<sup>1</sup>, Mauricio Calderón<sup>3</sup>, and Stephan A. Graham<sup>1</sup>

<sup>1</sup>*Department of Geological and Environmental Sciences, Stanford University, Stanford, California 94305, USA*

<sup>2</sup>*Chevron Energy Technology Company, San Ramon, California 94583, USA*

<sup>3</sup>*Departamento de Geología, Universidad de Chile, Casilla 13518, Correo 21, Santiago, Chile*

## ABSTRACT

The kinematic evolution of the Patagonian fold-and-thrust belt and cogenetic Magallanes retroarc foreland basin is reconstructed using new geologic mapping, two-dimensional (2-D) seismic-reflection data, and zircon U/Pb geochronology. Results span an ~160-km-wide transect of the thrust belt and Magallanes Basin near 51°30'S and highlight the influence of inherited extensional structures on basin paleogeography, syntectonic sedimentation, and Late Cretaceous–Neogene foreland shortening. South of 50°S, the Patagonian fold-and-thrust belt developed on oceanic and attenuated crust of the predecessor Late Jurassic Rocas Verdes rift basin, resulting in a collisional nature to early fold-and-thrust belt development and foreland sedimentation atop rifted South American crust.

We identify six principal stages of development between Late Cretaceous and Neogene time. A palinspastic restoration indicates ~32–40 km (~19%–23%) of retroarc shortening following closure of the Rocas Verdes Basin and incipient growth of the thrust belt. More than half of the estimated crustal shortening occurred synchronously with the deep-water phase of Late Cretaceous foreland basin sedimentation. Subsequent deformation migrated into the foreland, accounting for ~12 km of shortening across the Cretaceous–early Miocene basin fill. Thick-skinned thrust faulting along multiple detachment levels in Paleozoic metamorphic basement resulted in ~5 km of foreland uplift and exposure of preforeland basin deposits. The final phase of early Miocene deformation ca. 21–18 Ma may reflect enhanced coupling between the continental and oceanic lithospheres, causing

foreland basement uplifts as the Chile Ridge spreading ridge approached the trench. We speculate that Neogene foreland shortening was accommodated by reactivation of Mesozoic normal faults zones and accounts for broad uplift of the Patagonian fold-and-thrust belt.

## INTRODUCTION

Retroarc fold-and-thrust belts exemplify a dynamic balance among lithospheric convergence, thrust loading, topographic development by crustal thickening and arc emplacement, erosion, and foreland sedimentation. Substantial progress has been made in understanding the important roles of crustal shortening and lithospheric flexure (e.g., Jordan, 1981; Davis et al., 1983; Dahlen, 1990; Watts, 1992), synorogenic depositional architecture (e.g., DeCelles and Giles, 1996; Watts, 1992; Garcia-Castellanos, 2002; DeCelles, 2004), and erosion and exhumation in orogenic development (e.g., Beaumont et al., 1992; Willett, 1993; Hilley et al., 2005). However, most retroforeland thrust belt models are largely based on data from orogens that developed on average-thickness (34–40 km) continental lithosphere, such as the Central Andes or Western U.S. Cordillera (Christensen and Mooney, 1995). In contrast, retroarc thrust belts and their linked foreland basins that develop in marine settings, typified by the incipient backarc thrusting in the modern Sea of Japan (Celaya and McCabe, 1987; Ingle, 1992), exhibit important stratigraphic (e.g., Romans et al., 2009b) and topographic differences (e.g., Royden and Karner, 1984; Desegaulx et al., 1991; Matenco et al., 2003) that are poorly understood in a continental framework (e.g., Flemings and Jordan, 1990; DeCelles and Mitra, 1995).

In some cases, the flysch stage of marine sedimentation associated with successor foreland basins is characterized by a prolonged period of

deep-water (e.g., >1500 m deep) deposition, in addition to the presence of a submerged thrust belt composed of dense crustal blocks (Wilson, 1991; Sanders et al., 1999; Fildani and Hessler, 2005; Romans et al., 2009b). Additionally, provenance records of retroarc successor basins that evolve after ocean basins close can reflect the complex history of collision, alluding to mixed source terranes and reactivation of rift structures or terrane boundaries during contractional deformation (e.g., Graham et al., 1993; Fildani and Hessler, 2005). These attributes are difficult to reconcile with traditional retroforeland basin (Dickinson, 1976; DeCelles and Giles, 1996) and thrust belt models (Jordan, 1981) for continental-type orogenic belts. Although the opening and closing of backarc basins are fundamental aspects of convergent margin geodynamics (Dewey and Bird, 1970; Tamaki and Honza, 1991), relatively little is known about the ways in which aspects such as critically tapered wedge dynamics and basin histories may differ in fold-and-thrust belts that develop in deep-marine settings atop transitional crust. This discrepancy necessitates additional efforts to quantify and fully understand the controlling factors in the evolution of collisional retroarc fold-and-thrust belt and foreland basin systems.

The Cretaceous–Neogene Patagonian fold-and-thrust belt and Magallanes retroarc basin of southernmost South America (Fig. 1) developed on quasi-oceanic and attenuated continental crust of the predecessor Late Jurassic Rocas Verdes backarc basin (Katz, 1963; Dalziel et al., 1974; Fildani and Hessler, 2005). This convergent retroforeland system is perhaps the best type-example of such a unique basin configuration (e.g., Marsaglia, 1995; Romans et al., 2011), and recent studies of its synorogenic stratigraphic architecture have advanced our understanding of successor retroforeland basins, drawing upon the detrital record to reconstruct the orogenic history of the cogenetic thrust belt (Fildani and Hessler,

<sup>†</sup>E-mail: [julief@stanford.edu](mailto:julief@stanford.edu)

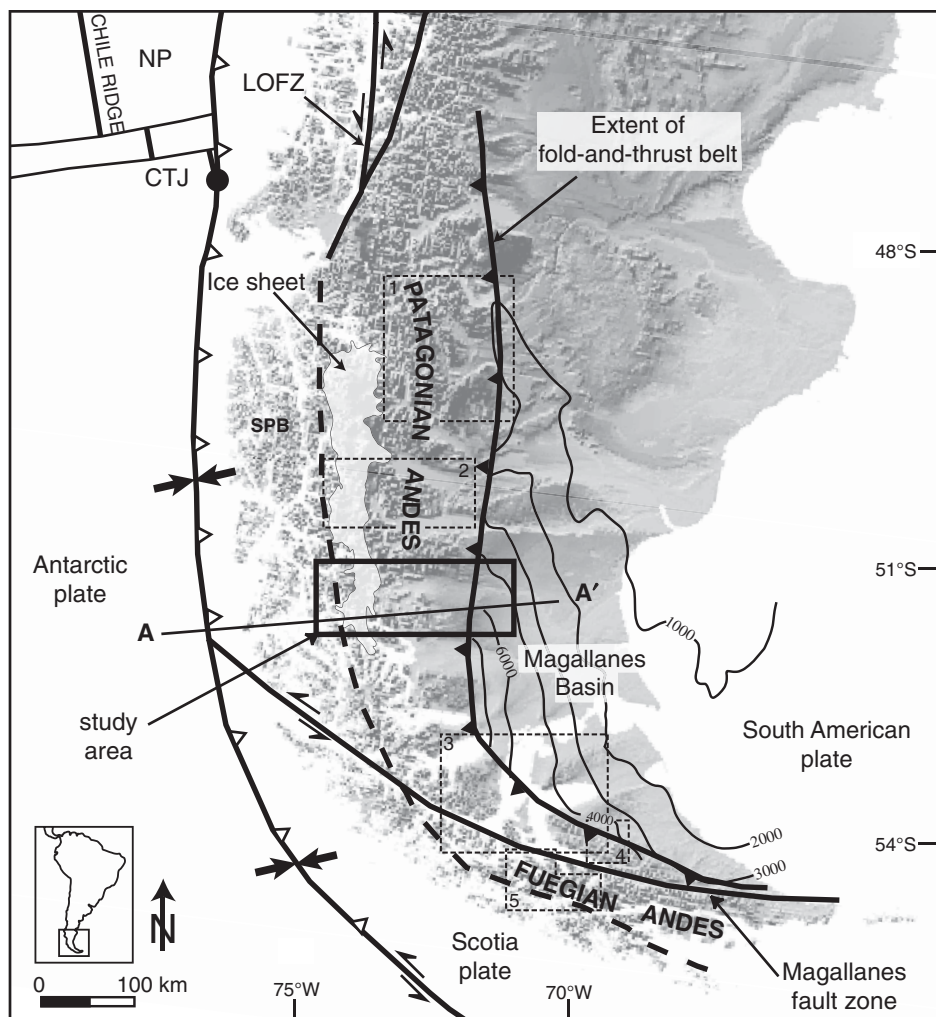


**Figure 1.** Tectonic setting of the Patagonian Andes, showing configuration of the Antarctic, Nazca, Scotia, and South American plates (modified from Thomson et al., 2001; Fildani and Hessler, 2005). The study area in Figure 3A is indicated by the bold black box and includes the Cordillera de los Andes, the Patagonian fold-and-thrust belt, and Magallanes retroforeland basin. The structure of the Patagonian margin along cross section A-A' is shown in Figure 2. Thin black boxes show location of selected published structural studies: (1) Ramos (1989), (2) Kraemer (1998) and Coutand et al. (1999), (3) Winslow (1982), (4) Alvarez-Marrón et al. (1993), (5) Klepeis et al. (2010). Black contours show depth to the Jurassic volcanic basement rocks, after Biddle et al. (1986). CTJ—Chile triple junction, LOFZ—Liquiñe-Ofqui fault zone, SPB—Southern Patagonian Batholith, and NP—Nazca plate. Base hillshade map was constructed from an SRTM 90 m digital elevation model.

2005; Ghigliione and Ramos, 2005; Olivero and Malumián, 2008; Fildani et al., 2009; Romans et al., 2009a, 2010). In this context, the Patagonian fold-and-thrust belt and Magallanes Basin afford an opportunity to characterize the structural style, thrust-front propagation rates, and associated sedimentation patterns in a collisional retroarc fold-and-thrust belt.

This paper describes foreland basin stratigraphic architecture, thrust-belt structures, and unpublished industry subsurface data from across the Andean orogen in Chile and Argen-

tina (Fig. 2) to characterize foreland deformation and cogenetic sedimentation history in a collisional retroforeland thrust belt that developed upon closure of the Rocas Verdes backarc basin. New zircon U/Pb ages from the sedimentary succession and crosscutting intrusions further refine the timing of deformation. We propose a kinematic history of deformation and identify six principal developmental stages in the Patagonian fold-and-thrust belt, drawing upon the robust stratigraphic record of Magallanes Basin evolution. While several key structural recon-

structions have been published from the northern segment of the Patagonian Andes, between 48°S and 50°S (Ramos, 1989; Kraemer, 1998; Coutand et al., 1999), and Fuegoian Andes, south of 52°S (Winslow, 1982; Alvarez-Marrón et al., 1993; Klepeis and Austin, 1997; Klepeis et al., 2010), this study fills a critical spatial gap in quantifying deformation across the entire retroforeland at 51°30'S.

## GEOLOGIC SETTING

The study area is located in the Patagonian Andes near 51°30'S, south of the present-day Chile triple junction, where the Antarctic plate presently subducts beneath the South American margin (Fig. 1). The Andean orogen forms a pronounced, narrow topographic feature in contrast to the broad, high-elevation Cordillera in the Central Andes. The cross section in Figure 2 depicts the structure of the entire Andean orogenic belt and synthesizes regional crustal structure (Robertson et al., 2003; Lawrence and Wiens, 2004; Polonia et al., 2007) with data from the batholith (Hervé et al., 2007b), fold-and-thrust belt, and Magallanes foreland basin structure (this study). The study area resides in an important position in the Patagonian Andes, because (1) it transects the northern extent of the quasi-oceanic Rocas Verdes rift basin and associated ophiolitic complexes, and (2) it captures the geometry of thrusting within the deep-marine portion of the Magallanes Basin (Fig. 1) (Natland et al., 1974). North of this study area, existing structural studies characterize foreland shortening across mildly attenuated continental crust (Ramos, 1989; Kraemer, 1998) associated with shallow and nonmarine foreland basin facies (Natland et al., 1974; Biddle et al., 1986; Macellari et al., 1989).

The Chile Trench is characterized by a forearc accretionary prism above the subducting oceanic plate (Fig. 2) (Polonia et al., 2007). Inboard of the Chile Trench, the Southern Patagonian Batholith consists of Jurassic through Neogene plutons (Hervé et al., 2007a) that intrude Paleozoic metamorphic basement (Forsythe and Mpodozis, 1979; Allen, 1982; Pankhurst et al., 2003; Hervé et al., 2003) and an Andean fold-and-thrust belt (Fig. 2). Farther east, the Patagonian fold-and-thrust belt consists of remnants of the Late Jurassic marginal Rocas Verdes Basin (Katz, 1963; Dalziel, 1981; Allen, 1982; Wilson, 1991; Fildani and Hessler, 2005; Calderón et al., 2007a) and the sedimentary fill of the Upper Cretaceous–Neogene Magallanes retroforeland basin (Fig. 3A<sup>1</sup>) (Katz, 1963; Biddle et al., 1986;

<sup>1</sup>Figure 3 is on a separate sheet accompanying this issue.

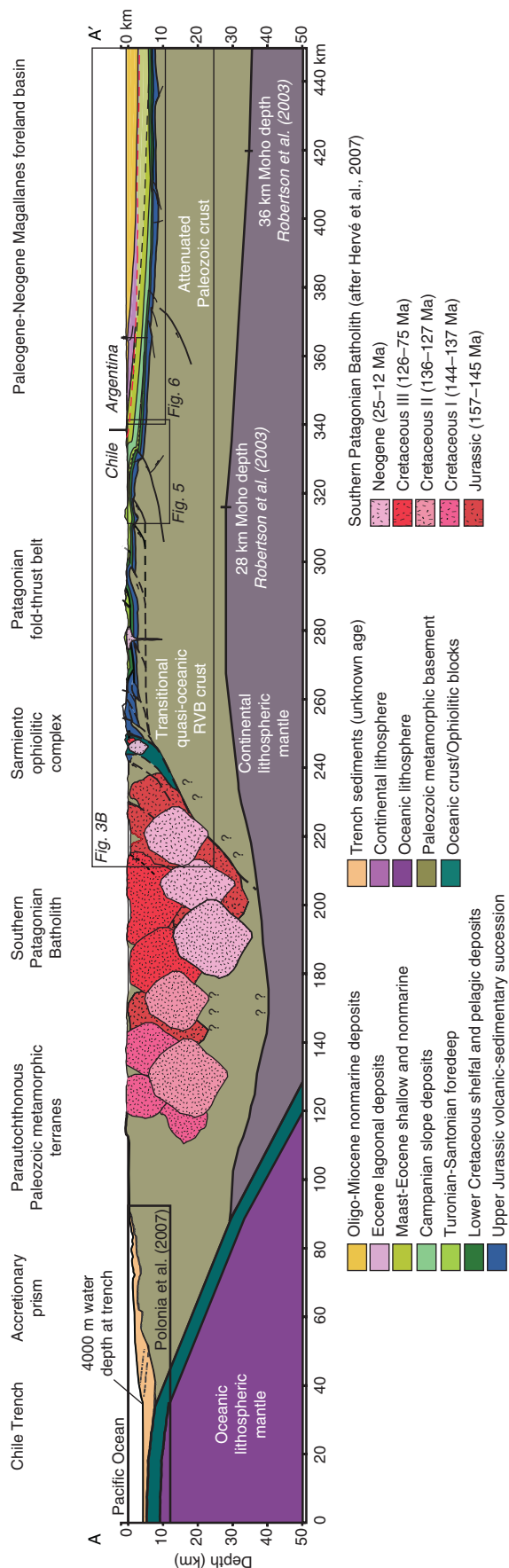


**Figure 2.** Structural cross section A-A' from Figure 1 of the Andean margin at 51°30'S, showing the forearc region (after Polonia et al., 2007), the Southern Patagonian Batholith (schematically shown following intrusive ages from Hervé et al., 2007b), uplifted Paleozoic metamorphic basement, the Sarmiento ophiolite complex, the Patagonian fold-and-thrust belt, and Magallanes foreland basin. Lithospheric structure beneath the thrust belt and foreland region is based on geophysical studies by Robertson et al. (2003) and Lawrence and Wiens (2004) and extrapolated beneath the magmatic arc. RVB—Rocas Verdes Basin.

Wilson, 1991; Malumián and Caramés, 1997; Fildani et al., 2008; Romans et al., 2011). Available geophysical studies elucidate the lithospheric structure of the foreland and suggest a Moho depth of  $28 \pm 3$  km, which deepens eastward to  $36 \pm 3$  km (Fig. 2) (Robertson et al., 2003; Lawrence and Wiens, 2004). This apparent westward crustal thinning beneath the fold-and-thrust belt may be the result of Neogene slab-window asthenospheric upwelling (Gorring et al., 1997; Breitsprecher and Thorkelson, 2009) and/or reflect crustal attenuation during Late Jurassic rifting (Dalziel, 1981).

### Rocas Verdes Marginal Basin History

During the breakup of Gondwana in Middle to Late Jurassic time (Pankhurst et al., 2000), the southern Patagonian Andes underwent crustal extension that culminated in the opening of the marginal Rocas Verdes Basin (Dalziel and Cortés, 1972; Suárez, 1979; Dalziel, 1981). This marginal basin widened southward from its inferred northern limit near 50°S, reflecting higher magnitudes of extension and partial melting of the lithosphere (Dalziel et al., 1974; De Wit and Stern, 1981; Allen, 1982). In eastern Patagonia, the Rocas Verdes Basin is composed of attenuated Paleozoic basement and synrift volcanic and volcanoclastic rocks of the Tobífera Formation (Figs. 3 [see footnote 1] and 4) (Suárez and Pettigrew, 1976; Fildani and Hessler, 2005). Crustal thinning and bimodal magmatism progressed in the western and southern parts of the basin and resulted in mid-ocean-ridge magmatism, represented by the Sarmiento and Tortuga ophiolitic complexes (Stern, 1980; Allen, 1982; Alabaster and Storey, 1990; Calderón et al., 2007a). The Rocas Verdes ophiolites (Stern and de Wit, 2003) preserve dismembered sections of the lateral lithologic transition from continental rifting to seafloor spreading and developed in a suprasubduction environment. As with many of the Cordilleran-type ophiolites, the Sarmiento ophiolitic complex shows an incomplete ophiolite pseudostratigraphy: It has well-preserved mafic upper extrusive units and bimodal magmatic suites, but it is missing ultramafic or mantle rocks (e.g., Pearce, 2003). As such, the Sarmiento ophiolitic complex is interpreted to represent transitional quasi-oceanic crust of the Rocas Verdes rift basin (Calderón et al., 2007b).

The restricted outcrop preservation and subsequent deformation of the Rocas Verdes Basin preclude a reliable reconstruction of maximum marginal basin width. Dalziel (1981) evaluated the relative melt generation between bimodal magmatism (e.g., Stern, 1980; McKenzie and Bickle, 1988) in the Sarmiento and Tortuga ophiolitic complexes and concluded that the

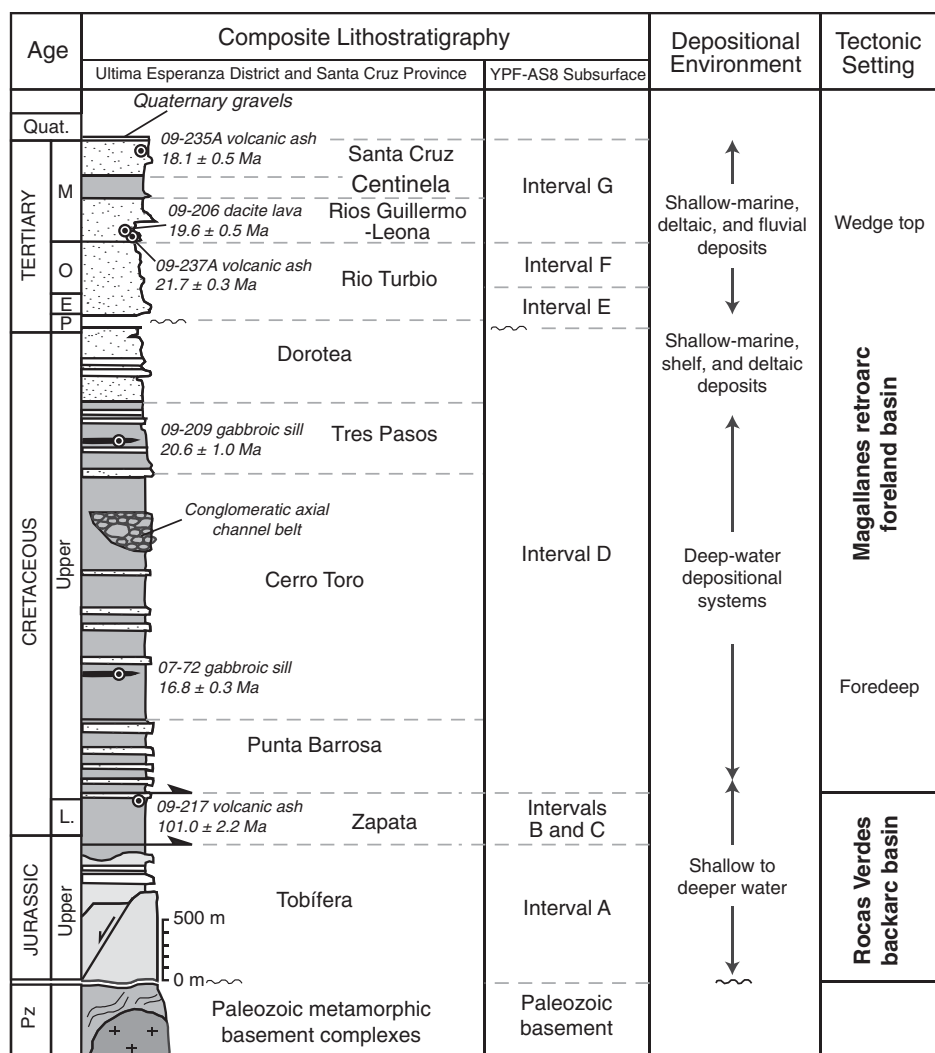


**Figure 4.** Generalized composite stratigraphic section for the Rocas Verdes and Magallanes Basins in the Ultima Esperanza District, Chile, and Santa Cruz Province, Argentina. Stratigraphic thicknesses and depositional environments are compiled from Katz (1963), Natland et al. (1974), Wilson (1983), Malumián et al. (2001), Fildani and Hessler (2005), Hubbard et al. (2008), Covault et al. (2009), and Romans et al. (2009a). Subsurface stratigraphic intervals, interpreted in seismic-reflection line YPF-AS8 (Fig. 6), are broadly correlated to the outcrop stratigraphy shown in the left-hand column. New zircon U/Pb ages and sample locations from interbedded volcanic ash layers and crosscutting gabbroic sills are shown.

basin was at least 50 km wide in the north and upward of 100 km in Tierra del Fuego. This basin configuration, though smaller, is analogous to the present-day Sea of Japan marginal basin, which is ~850 km wide and is structurally partitioned into continental basement blocks and a restricted area of quasi-oceanic crust (e.g., Celaya and McCabe, 1987; Ingle, 1992).

As extension waned, the Rocas Verdes Basin accumulated fine-grained sediments of the Lower Cretaceous Zapata Formation (Fig. 3A [see footnote 1]), originating from local basement uplifts with input from a juvenile volcanic arc to the west (Fildani and Hessler, 2005). Early Creta-

ceous sedimentation and subsidence proceeded for nearly 20 m.y. before the onset of foreland basin sedimentation (Fildani et al., 2003; Fildani and Hessler, 2005; Calderón et al., 2007a).

#### Retroforeland Convergence and Magallanes Basin Evolution

During Early Cretaceous time, increased rates of spreading in the South Atlantic Ocean and accelerated subduction rates along the Pacific margin (Rabinowitz and La Brecque, 1979; Dalziel, 1986; Ramos, 1989) are thought to have caused the transition from extension to

compression in the retroarc region of the Patagonian Andes, thereby initiating Rocas Verdes Basin closure (e.g., Bruhn and Dalziel, 1977; Hervé et al., 2007b). Thrust loading of dense oceanic crustal blocks resulted in a stage of deep-water sedimentation in the narrow and elongate foredeep of the Magallanes foreland basin (Natland et al., 1974; Winn and Dott, 1979; Dalziel, 1981; Wilson, 1991; Fildani and Hessler, 2005; Romans et al., 2009b) that was well developed by 92 Ma (Fildani et al., 2003). Deep-marine sedimentation persisted with deposition of >2000 m of the mud-rich Cerro Toro Formation (Fig. 4). During this time, denudation of the hinterland fed conglomerate-filled channels in the axial foredeep of the basin (Fig. 3A [see footnote 1]) (Scott, 1966; Natland et al., 1974; Winn and Dott, 1979; Crane and Lowe, 2008; Hubbard et al., 2008). Continued Late Cretaceous deposition in the deep-water environment resulted in basin filling and southward slope progradation of the Tres Pasos Formation (Fig. 4) (Biddle et al., 1986; Armitage et al., 2009; Romans et al., 2009a; Hubbard et al., 2010) and shoaling upward to shallow-marine and deltaic facies of the Maastrichtian–Danian Dorotea Formation (Figs. 3A [see footnote 1] and 4) (Macellari et al., 1989; Fildani et al., 2008; Covault et al., 2009; Romans et al., 2011).

Paleocene uplift and deformation of the Cretaceous foreland basin fill have been previously suggested, based on an erosional unconformity spanning nearly 15 m.y. near the base of the Tertiary basin fill (Figs. 3A [see footnote 1] and 4) (Malumián et al., 1999). In the Santa Cruz Province of Argentina (Fig. 3A [see footnote 1]), this unconformity is represented by Maastrichtian–Danian (?) shallow-marine strata of the Dorotea Formation overlain by the Eocene lagoonal Rio Turbio Formation (Fig. 4) (Malumián and Caramés, 1997). Syntectonic deposition continued farther east in the foreland through early Miocene time, resulting in shallow-marine, estuarine, and lagoonal growth strata along the eastern margin of the thrust belt (Fig. 4) (Riccardi and Rolleri, 1980; Malumián and Caramés, 1997; Malumián et al., 2001; Parras et al., 2008). The stratigraphic section in the Santa Cruz Province is capped by the widespread fluvial deposits of the Miocene Santa Cruz Formation (Fig. 3A [see footnote 1]) (Ramos, 1989; Malumián et al., 2001; Blisniuk et al., 2005).

#### METHODOLOGY

##### Subsurface Stratigraphic Analysis

The structure and regional stratigraphic architecture were constrained by regional two-dimensional (2-D) seismic-reflection data from

Empresa Nacional del Petróleo-Sipetrol (ENAP-Sipetrol) and Repsol Yacimientos Petrolíferos Fiscales Sociedad Anónima (Repsol YPF S.A.) (Figs. 5 and 6). These data provide a view into the nature of the frontal thrust faults in the Andean thrust belt and the broader stratigraphic architecture of the Magallanes Basin. Seismic stratigraphic intervals, reflector terminations, and structures were interpreted from migrated seismic-reflection data in seismic two-way traveltime (s) (Figs. 5 and 6) and aided our regional characterization of the subsurface thrust belt (Fig. 3B [see footnote 1]). More than 15 seismic-reflection lines from Repsol S.A. and ENAP-Sipetrol, acquired between 1978 and 1988, were evaluated in this study, and the most complete data set that coincided with our structural transect is presented here (YPF-AS8 and ENAP-5004). To incorporate the seismic-

reflection data into our structural cross section, we performed a depth conversion using a bulk velocity model of 2.5 km/s for compacted sedimentary rocks (Blatt, 1979), and calibrated this conversion with sedimentary isopach maps and the depth-to-basement model of Biddle et al. (1986). Stratigraphic ages within the subsurface data from well YPF-SC-1 were interpreted from proprietary Repsol YPF S.A. core data and correlated to outcrop micropaleontology studies (Natland et al., 1974; Dott et al., 1977).

### Structural Analysis

We integrated subsurface data with 1:100,000 scale geologic mapping (Fig. 3A [see footnote 1]) of the Patagonian fold-and-thrust belt to construct an incrementally restored, balanced cross section between the Sarmiento ophiolitic

complex and the undeformed foreland basin (Fig. 3B [see footnote 1]). The geologic map builds upon pioneering mapping by Wilson (1983) and others (Stewart et al., 1971; ENAP, 1978; Allen, 1982; Soffia et al., 1988; Malumián et al., 2001; Fildani and Hessler, 2005; Calderón et al., 2007a). Stratigraphic unit thicknesses were compiled from the work of Katz (1963), Winn and Dott (1979), Macellari et al. (1989), Wilson (1991), Malumián et al. (2001), Fildani and Hessler (2005), Hubbard et al. (2008), Armitage et al. (2009), and Covault et al. (2009). We take into account the observed stratigraphic thickening of the Upper Cretaceous units toward the foredeep by extrapolating from outcrop to subsurface geometries constrained by well data and 2-D seismic-reflection interpretations. A balanced structural cross section (Fig. 3B [see footnote 1]) was prepared following the methods of Dahlstrom (1969) and Suppe (1983). Sequential kinematic restorations of this cross section were performed using LithoTect™ flexural slip and line balancing methods (Dahlstrom, 1969; Suppe, 1983; Tanner, 1989; Lisle, 1992). Frontal thrust faults, foreland basin geometry, and rifted Paleozoic basement are based on interpretations of regional 2-D seismic-reflection data (Figs. 5 and 6).

### Zircon U/Pb Geochronology

Zircon U/Pb geochronology of interbedded volcanic ash and lava flows and crosscutting igneous intrusions provides a useful means with which to date the age of synorogenic deposition and basin deformation. By inference, the timing of thrust belt deformation associated with the synorogenic sedimentation can also be assessed using these age constraints (Fildani et al., 2003). We present zircon U/Pb data from six samples (Table 1), including interbedded volcanic ash, a dacite lava flow, and crosscutting gabbroic sills (Fig. 7). Zircon U/Pb ages from crystal rims were obtained for these samples on the sensitive high-resolution ion microprobe–reverse geometry (SHRIMP-RG) at the Stanford University–U.S. Geological Survey (USGS) facility (see GSA Data Repository for analytical methods<sup>2</sup>). Concordant <sup>207</sup>U-corrected <sup>206</sup>Pb/<sup>238</sup>U ages were calculated using Squid and Isoplot/Excel (Ludwig, 2000). In order to evaluate age populations that can be interpreted as eruptive or shallow-level intrusive ages of hypabyssal rocks, zircon U/Pb results were evaluated using the TuffZircon algorithm of Isoplot (Fig. 8)

<sup>2</sup>GSA Data Repository item 2011194, zircon U/Pb analytical procedures and supplemental data, is available at <http://www.geosociety.org/pubs/ft2011.htm> or by request to [editing@geosociety.org](mailto:editing@geosociety.org).

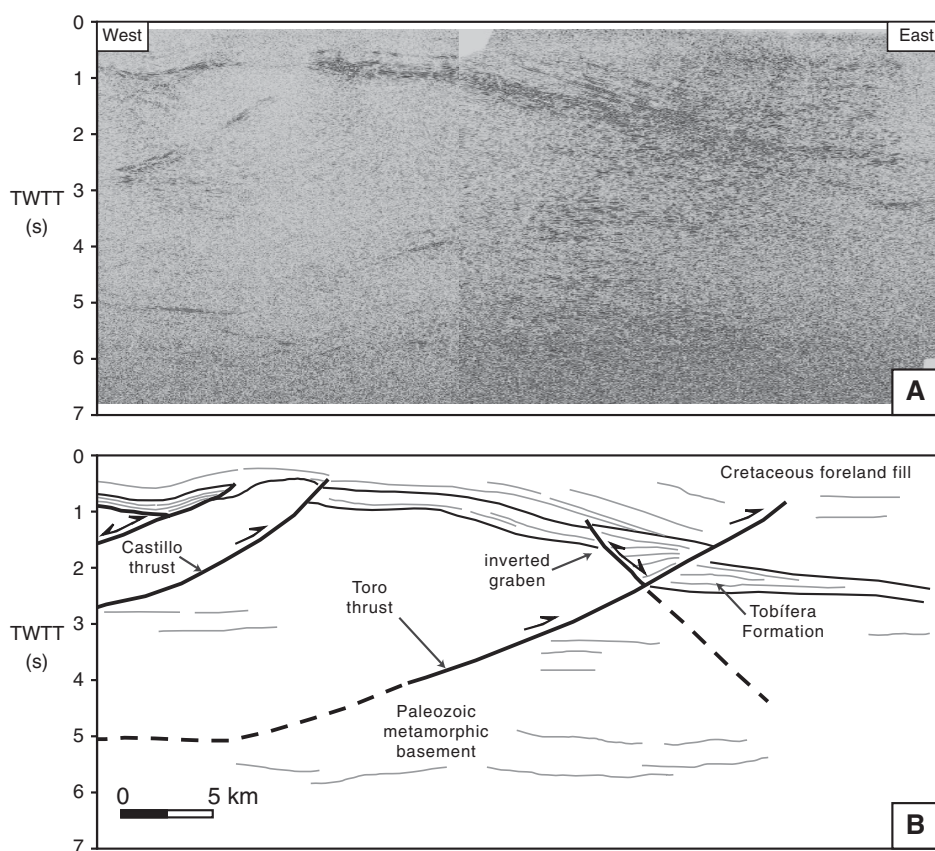


**Figure 5.** (A) Regional two-dimensional (2-D) seismic-reflection data from line ENAP-5004 across the frontal thrusts of the Patagonian fold-and-thrust belt (4× vertical exaggeration). Refer to Figure 3A for location of the seismic-reflection line. Data courtesy of Empresa Nacional del Petróleo-Sipetrol (ENAP-Sipetrol). (B) Line drawing interpretation of the stratigraphy and structure of line ENAP-5004, showing broad uplift and folding of the Tobifera Formation and Paleozoic metamorphic basement (after Harambour, 2002). High-angle thrust faults, informally named the Castillo thrusts and Toro thrust, are interpreted to sole out along basal detachments within the basement, near 3 and 5 s two-way traveltime (TWTT), respectively (e.g., Harambour, 2002).

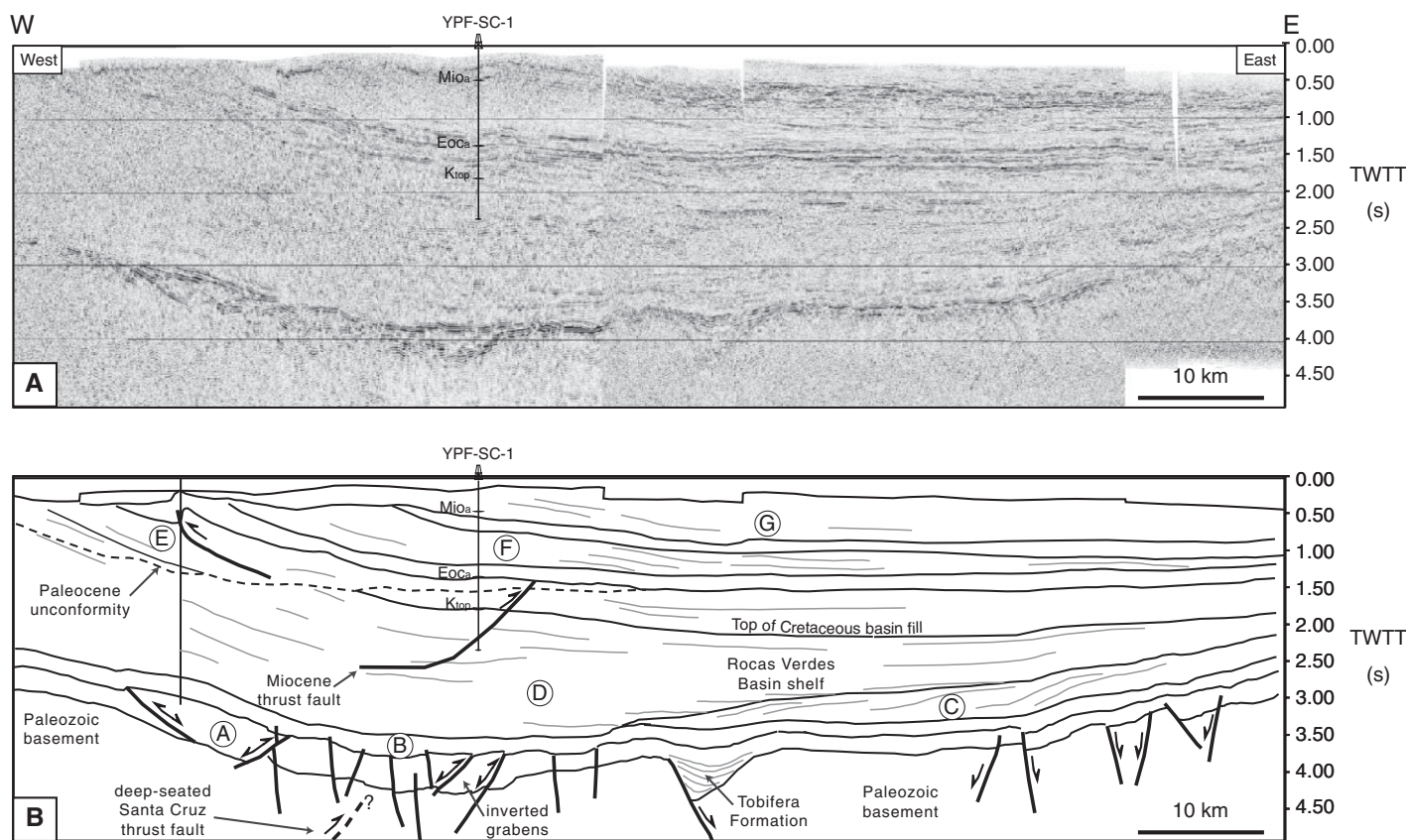


**Figure 6.** (A) Regional two-dimensional (2-D) seismic-reflection data from line YPF-AS8 across the Magallanes Basin (4× vertical exaggeration). Refer to Figure 3A for location of the seismic-reflection line. Data are courtesy of Repsol Yacimientos Petrolíferos Fiscales Sociedad Anónima (Repsol YPF). (B) Line drawing interpretation of the stratigraphy and structure of line YPF-AS8, showing rifted Paleozoic basement, synrift minibasins in-filled by Tobífera volcanoclastic rocks, and the Upper Cretaceous–Neogene foreland basin fill. Uplift and tilting of the basin fill and Paleozoic basement along the western margin of the basin allude to an underlying thrust fault that soles out along a basal detachment near 5 s two-way traveltime (TWTT), as depicted in Figure 3B. Stratigraphic intervals A through G are described in the text: A—Upper Jurassic Tobífera Formation; B—Lower Cretaceous Inoceramus Formation; C—eastern slope deposits of the Rocas Verdes Basin; D—Upper Cretaceous Magallanes foreland basin fill; E–G—Eocene through Miocene eastward-progradational foreland basin deposits.

(Ludwig, 2000). All zircon U/Pb isotopic data are reported in Table DR1, and summarized age data are shown in Figure 8. Zircon U/Pb results are presented within the following text in relation to the geologic context of each sample.

### STRUCTURE OF THE PATAGONIAN THRUST BELT

#### Sarmiento Ophiolitic Complex

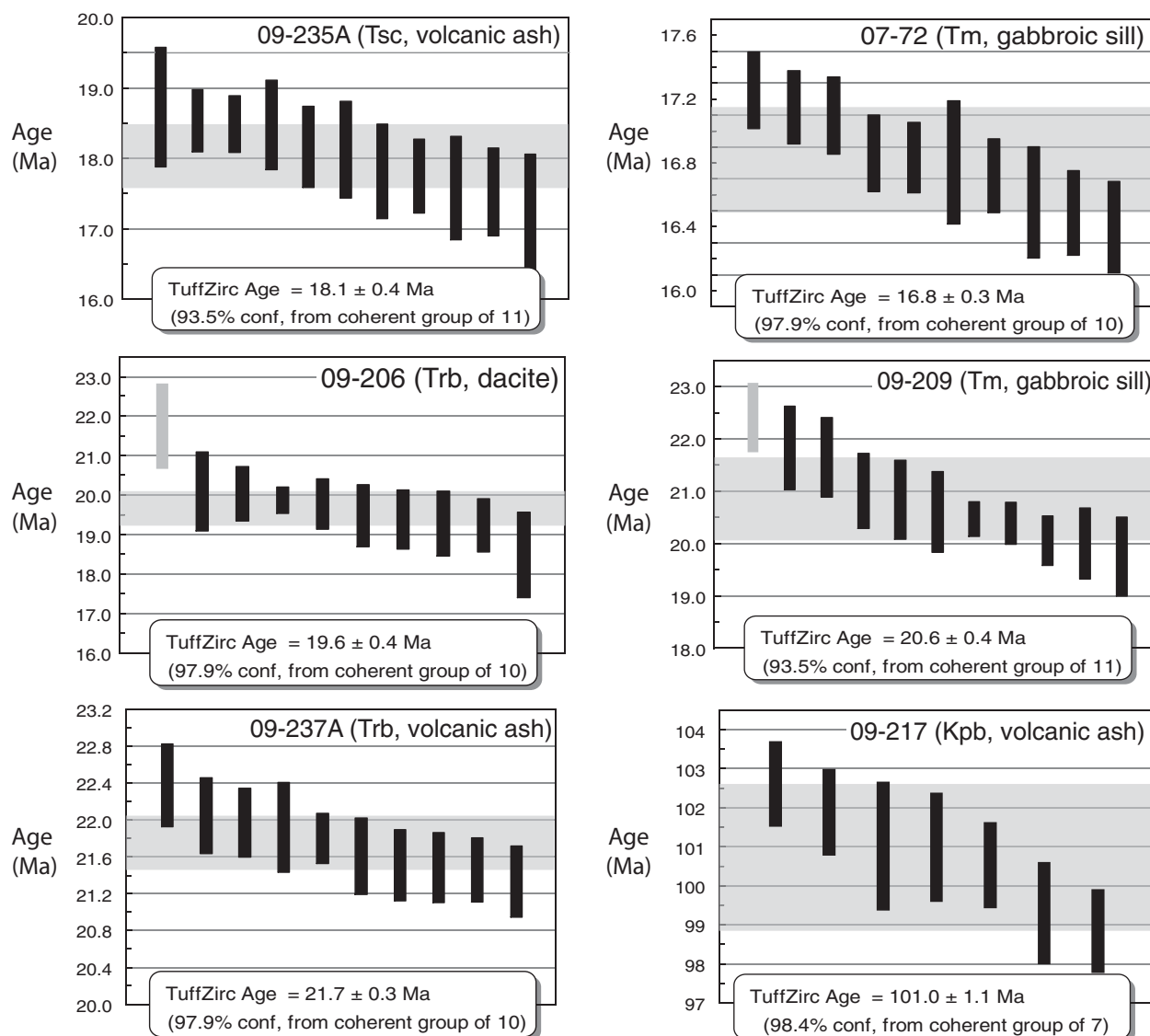
The earliest phase of Andean contractional deformation is recorded in the western outcrop belt of the Patagonian fold-and-thrust belt, where remnants of the quasi-oceanic Late Jurassic Rocas Verdes Basin are thrust eastward atop the Early Cretaceous clastic basin fill (Fig. 3A [see footnote 1]) (Allen, 1982; Calderón et al., 2007a). One of the most significant structures

TABLE 1. ZIRCON U/Pb SAMPLE INFORMATION

Sample	Latitude (°S)	Longitude (°W)	Elevation (m)	Formation	Lithology	<sup>207</sup> Pb <sub>corr</sub> / <sup>206</sup> Pb/ <sup>238</sup> U age (±1σ, Ma)
07-72	51°03.022'	73°04.786'	252	Mafic intrusive	Gabbro	16.9 ± 0.2
09-217	50°49.234'	72°22.087'	37	Punta Barrosa	Volcanic ash	101.0 ± 1.1
09-206	50°58.336'	72°35.465'	1053	Rio Guillermo	Dacite	19.7 ± 0.4
09-209	51°19.931'	72°48.680'	104	Mafic intrusive	Gabbro	20.6 ± 0.4
09-235A	51°26.839'	72°06.409'	814	Santa Cruz	Volcanic ash	18.1 ± 0.4
09-237A	51°18.203'	72°11.202'	389	Rio Guillermo	Volcanic ash	21.7 ± 0.3

within the Rocas Verdes Basin suture, the Canal de las Montañas shear zone, juxtaposes oceanic crustal rocks of the Sarmiento ophiolitic complex against felsic volcanogenic rocks of the Tobífera Formation with a bulk reverse, west-over-east tectonic transport (Calderón et al., 2009). Estimates of shortening across this shear zone are difficult to assess because of the intense degree of deformation. Pressure solution

and solution transfer deformation mechanisms associated with the development of microstructures and synkinematic recrystallization of white mica, chlorite, and stilpnomelane (Galaz et al., 2005; Hervé et al., 2007a) in these highly strained rocks within the Canal de las Montañas shear zone indicate low-temperature (close to ~400 °C) conditions for mylonitic deformation in the presence of fluids.



**Figure 7.** Zircon U/Pb sensitive high-resolution ion microprobe–reverse geometry (SHRIMP-RG) ages ( $^{204}\text{Pb}$  corrected) from crystal rims, calculated using TuffZirc algorithm of Ludwig and Mundil (2002) in the Isoplot program (Ludwig, 2000). Samples include volcanic ash from the Tertiary Magallanes Basin fill and crosscutting gabbroic sills. Black boxes are the error bars ( $2\sigma$ ) for individual zircons analyzed, and gray boxes are for zircons not included in the median age calculated from the coherent group (due to possible Pb loss). Horizontal gray band shows the inferred age and uncertainty of the syngenetic zircons. Asymmetric uncertainties reflect complexity (e.g., Pb loss or xenocrystic behavior) in the direction of the larger error. For reporting the inferred syneruptive or crystallization ages, the largest of the two uncertainties is reported. Refer to Table 1 for sample information and GSA Data Repository for detailed analytical procedures (see text footnote 2).

#### **Zircon U/Pb Constraints on Initiation of Foreland Basin Sedimentation**

Late Cretaceous crustal shortening of the Paleozoic basement and Rocas Verdes Basin blocks in the western Cordillera de los Andes is generally accepted as having caused the initial flexural loading of the foreland (Dalziel, 1981; Wilson, 1991; Fildani and Hessler, 2005). In the Ultima Esperanza region, the predominance of thick (>1 m) turbidite sand beds in the Punta

Barrosa Formation reflects the presence of a well-developed subaerial fold-and-thrust belt by  $92 \text{ Ma} \pm 1.0 \text{ Ma}$  (Fildani et al., 2003).

We present new zircon U/Pb results from an interbedded volcanic ash (sample 09–217) collected below the basal member of the Punta Barrosa Formation, indicating an eruption age of  $101 \pm 1.0 \text{ Ma}$  (Figs. 3 and 7). The volcanic ash sample was collected from within the upper parts of the Zapata–Punta Barrosa transition

(cf. Fildani and Hessler, 2005), a gradational package of strata characterized by thin-bedded turbiditic sandstone and shale punctuated by isolated sand beds up to 40 cm thick. Fildani and Hessler (2005) documented increasing frequency of fine-grained turbidites composed of immature, poorly sorted sandstone with angular grains in the upper Zapata Formation and suggested that a young fold-and-thrust belt had developed toward the end of Zapata deposition

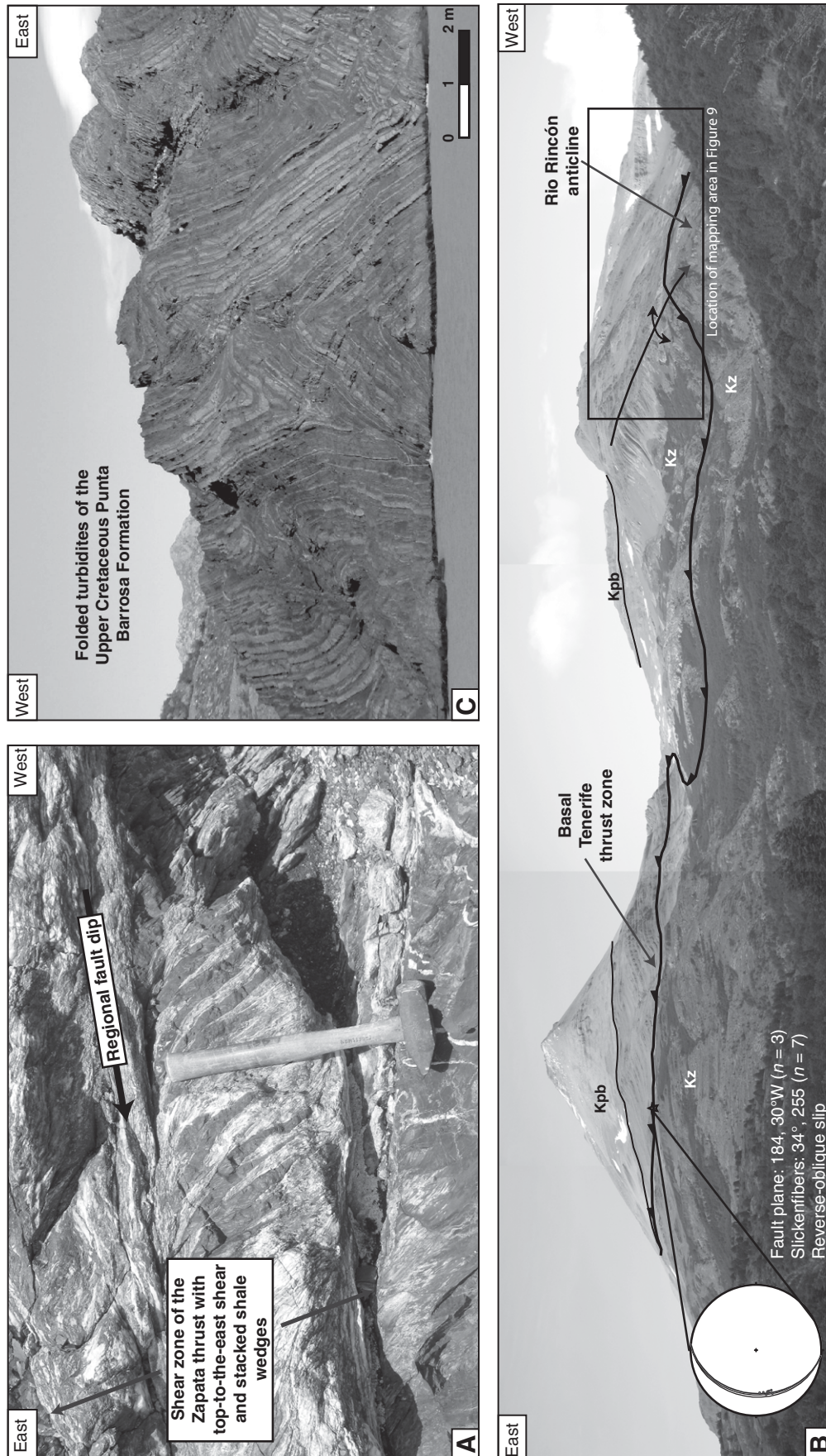


Figure 8. (A) Zapata thrust (cf. Wilson, 1983), developed at the base of the Zapata Formation. The thrust zone is overturned and gently west-dipping, with top-to-the-east reverse shear sense indicated by repeated shear wedges within the shear zone. (B) Oblique view of the Tenerife thrust fault and Rio Rincón anticline exposed along the northern flanks of Cerro Tenerife in the Cordillera Arturo Prat. The thrust flat shown here juxtaposes the Upper Cretaceous Punta Barrosa Formation above the underlying Lower Cretaceous Zapata Formation. To the east, this fault cuts up-section and produces tight folds in the Punta Barrosa Formation. (C) Faulted and folded turbidite beds of the Punta Barrosa foredeep deposits, exposed along the northwest shore of Lago Grey.

ca. 95 Ma. Our new U/Pb eruptive age of volcanic ash interbedded with these fine-grained turbidites is slightly older and provides additional information on the timing of incipient foreland basin formation and the earliest arrival of the coarse-grained sediments into the juvenile Magallanes Basin.

### Tobífera Hinterland Thrusts

The Cordillera de los Andes consists of the Tobífera thrust sheets (Fig. 3A [see footnote 1]), which are characterized by a major antiformal structure with steeply dipping domainal fabrics, localized subvertical shear zones (e.g., Allen, 1982; Galaz et al., 2005; Calderón et al., 2007a; Hervé et al., 2007b), and regional N-S subvertical penetrative cleavage (e.g., Wilson, 1983; Calderón et al., 2007a). Extensive cover from the Patagonian ice sheet limits a detailed study of the internal structure of the Tobífera thrust sheets, although existing mapping suggests that Paleozoic metamorphic complexes are involved in thrusting (Fig. 3B [see footnote 1]) (Allen, 1982). The westernmost exposure of the Tobífera Formation is in thrust contact with the contemporaneous Sarmiento ophiolitic complex, which has been obducted onto the South American margin and thrust over the Jurassic volcanoclastic succession along the Canal de las Montañas shear zone, described previously. This contact is interpreted as the surface exposure of the orogenic suture and culminating closure of the Rocas Verdes Basin (e.g., Calderón et al., 2009).

The structural relationships along the eastern edge of the Cordillera de los Andes exhibit a more complex geometry of Tobífera thrusting. West of the Torres del Paine massif (Fig. 3A [see footnote 1]), a shallowly east-dipping detachment between the Tobífera and overlying Zapata Formation exhibits top-to-the-east shear sense and reverse drag (Fig. 9A). Wilson (1983) first interpreted this fault—the “South Zapata thrust”—as a passive roof thrust to an antiformal stack of Tobífera imbricate thrusts that likely correlated to the high-angle shear zone within the Zapata and Tobífera Formations on the western flanks of the Cordillera de los Andes (Allen, 1982; Calderón et al., 2007a) (Fig. 3B [see footnote 1]). Extensive ice cover and limited accessibility restrict a more thorough study of this thrust zone along strike; nonetheless, fault geometry and shear sense indicators (Fig. 8A) corroborate the interpretation of a forward-dipping duplex for the Tobífera thrusts (Wilson, 1983).

The development of an antiformal duplex has substantial implications for high-magnitude shortening via vertically stacked thrust

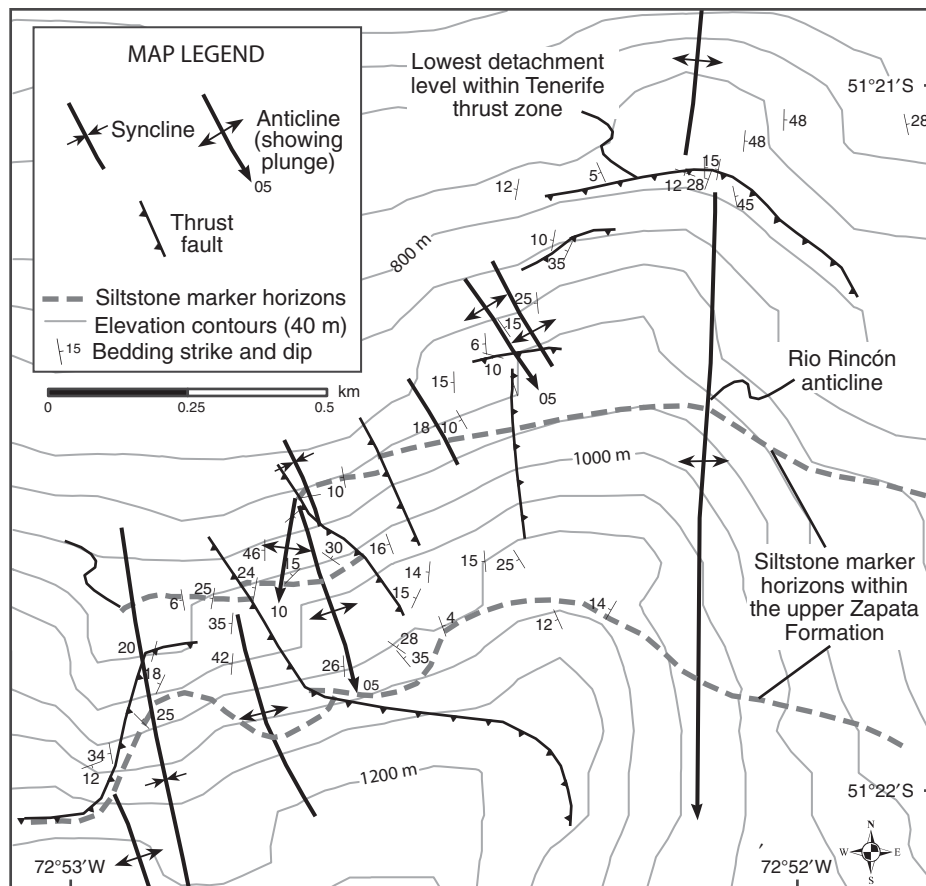


**Figure 9.** Geologic map of the Tenerife thrust zone, developed within the Zapata Formation west of Cerro Tenerife (for location, refer to Fig. 3A). The structure of two siltstone intervals (dashed gray lines) aids in defining the faults and folds in the Tenerife thrust zone. Palinspastic restorations of siltstone horizon line lengths indicate ~22% shortening over ~2.25 km distance.

sheets and a potentially large volume of uplifted material supplied to the coeval foreland basin. In the foliated Tobífera metarhyolite flows exposed in these thrust sheets, syntectonic metamorphic assemblages suggest tectonic burial to depths of ~15–20 km between 150 and 100 Ma (Galaz et al., 2005; Calderón et al., 2007a; Hervé et al., 2007b). This could easily be accomplished by stacking several thrust sheets via detachment faults that sole out in metamorphic basement, each having a thickness of ~5–8 km. We consider this valuable pressure-temperature (*P-T*) data in our structural interpretation and favor a duplex geometry (Fig. 3B [see footnote 1]), although this remains speculative without more robust outcrop and subsurface data from this remote part of the thrust belt.

The exact amount of shortening taken up within the Tobífera thrusts is ambiguous, and we propose a probable range of values given the following observations: (1) structurally re-

peated Tobífera Formation along an inferred detachment atop the Paleozoic basement, (2) the presence of a roof thrust of the South Zapata thrust and the overall antiformal geometry of the Cordillera de los Andes, and (3) the 15–20 km burial depth history of the Tobífera thrust sheets. These factors support an antiformal duplex geometry that yields ~27 km of shortening, reconstructed by bed length restoration of the Tobífera-Zapata depositional contact (Fig. 3B [see footnote 1]). In a more conservative end-member interpretation of simple imbricate thrust sheets, spaced 5–8 km apart (Galaz et al., 2005; Calderón et al., 2007a) and soling out in the same level of Paleozoic basement, restored line lengths suggest ~20 km of shortening. Given the limited accessibility, ice cover, and paucity of subsurface constraints beneath the Tobífera thrusts, these shortening estimates are the least constrained values for this study, and we use this 20–27 km range of values for the kinematic reconstruction (Fig. 10A).

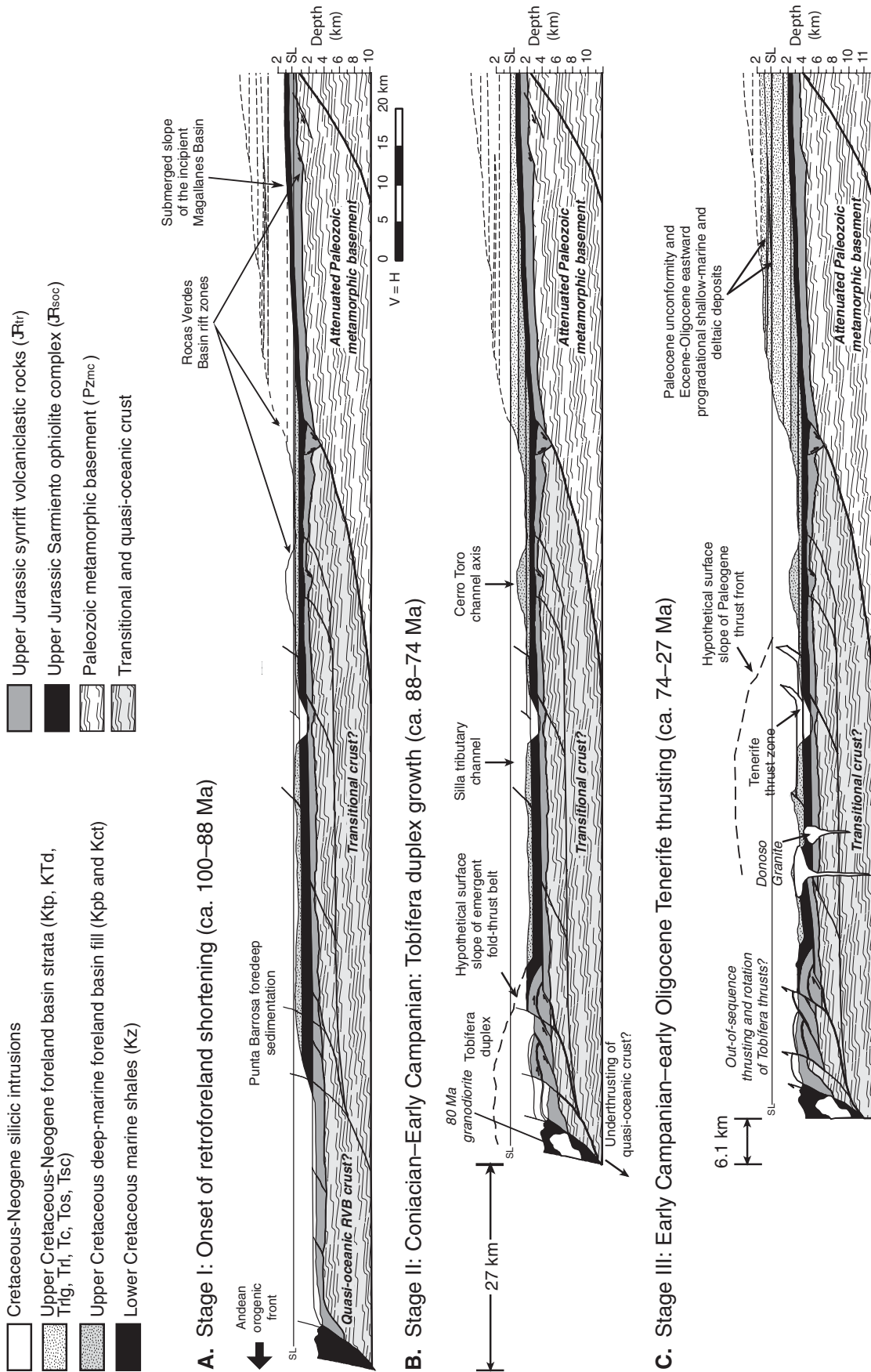


Figure 10 (on this and following page). Kinematic restoration of the Patagonian fold-and-thrust belt across line B-B' (Fig. 3A), showing progression of deformation and concurrent foreland basin evolution. In each stage, outlines of white geologic units have yet to be deposited and represent the extent of geologic data used in the palinspastic reconstruction. (A) Onset of retroforeland shortening and early foreland basin phase (ca. 100–88 Ma). The orogenic front is located to the west of the line of section. (B) Tobifera duplex growth and axial submarine drainage (ca. 88–74 Ma). (C) Tenerife thrusting and incorporation of Upper Cretaceous basin fill into the fold-and-thrust belt (ca. 74–27 Ma). SL—sea level; RVB—Rocas Verdes Basin.

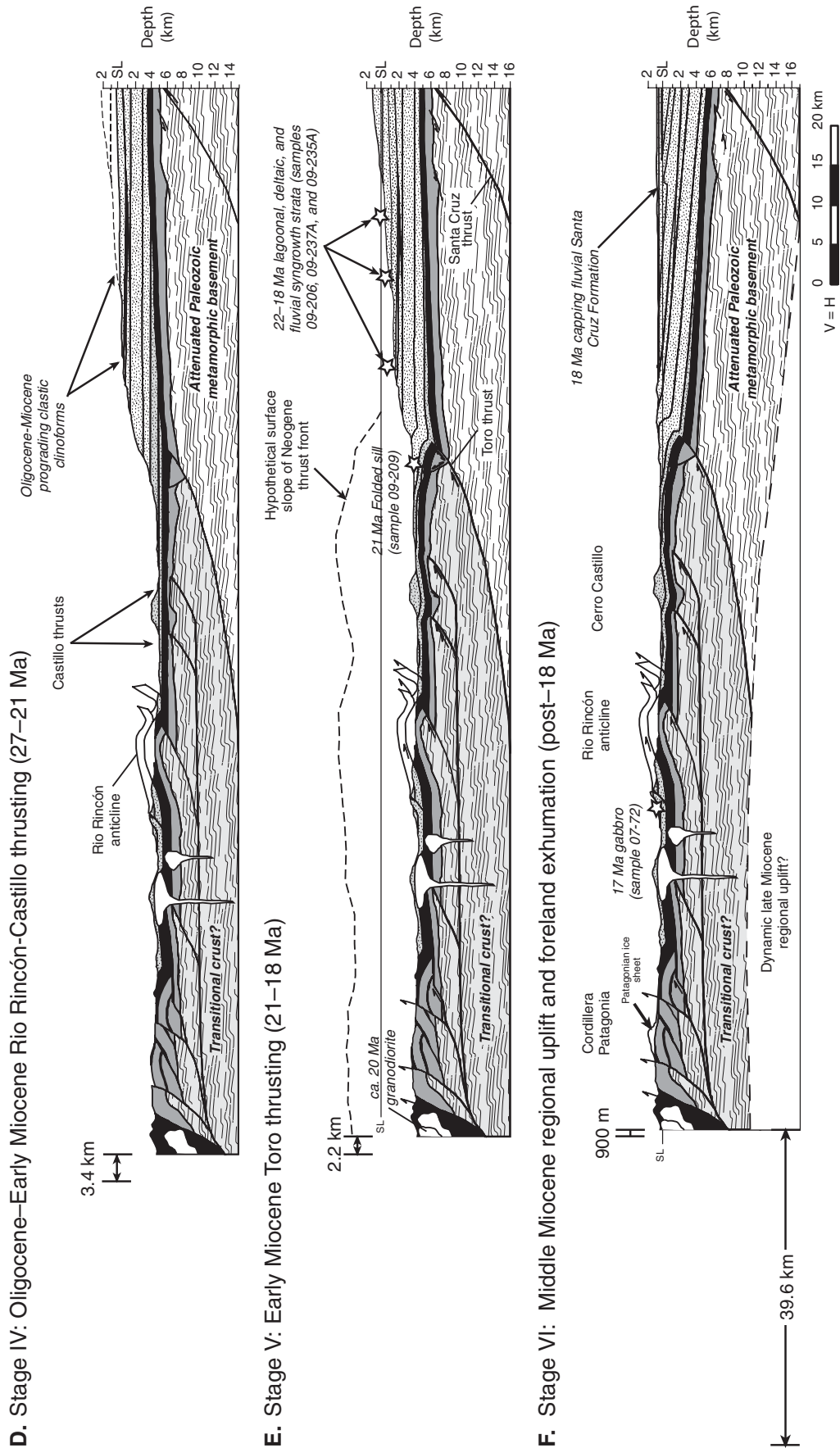


Figure 10 (continued). (D) Rio Rincón–Castillo thrusting and concurrent shallow-marine and deltaic sedimentation (ca. 27–21 Ma). (E) Toro thrusting and deepening of the basal detachment within Paleozoic basement (ca. 21–18 Ma). (F) Santa Cruz thrusting and regional uplift of Patagonia (post–18 Ma to present day).

## Tenerife Thrust Zone

Deformation along the western margin of the Cretaceous foreland basin has been accommodated by a thin-skinned thrust fault, here named the “Tenerife thrust zone” for its outcrop exposure on Cerro Tenerife (Figs. 3 [see footnote 1] and 8B). The upper plate of the Tenerife thrust zone is characterized by a 600-m-thick zone of thin-skinned thrust faults and related folds developed within the uppermost Zapata Formation (Fig. 9). This thrust sheet is ~30 km wide and encompasses open folds exposed on Cerro Balmaceda and in the Cordillera Arturo Prat (Fig. 3A [see footnote 1]). On Cerro Tenerife, one of the most prominent faults exhibits a gently west-dipping fault surface (184, 30°W) with quartz and calcite fibrolinements that plunge 34° toward the SSW, indicating a top-to-the-east shear sense (Fig. 8B). The Tenerife thrust zone accounts for structural thickening of the Zapata and Punta Barrosa Formations in the Cerro Balmaceda region, in addition to localized, tight folding where subsidiary faults cut up-section and displace Punta Barrosa strata on top of the stratigraphically younger Cerro Toro Formation (Fig. 3A [see footnote 1]). For example, the upper member of the Punta Barrosa Formation is juxtaposed against the middle Cerro Toro Formation along the Rio Nutria thrust (Wilson, 1983), indicating ~1 km of displacement on this subsidiary fault (Fig. 3A [see footnote 1]).

Given the limited exposure of thrust-fault flats and homogeneity of the shale-rich stratigraphy, it is difficult to assess the total slip along the Tenerife fault. Detailed mapping of the Tenerife thrust zone along the western flanks of Cerro Tenerife documents a series of five reverse faults and fault-bend folds within the Tenerife thrust zone that sole out in the Zapata shale beds (Fig. 9). Fault displacement and folding across a 2.25 km distance account for ~500 m shortening across (Fig. 10), indicating ~22% local strain. Since this magnitude and style of Tenerife thrust zone deformation extend across the full 30 km width of the Tenerife thrust sheet (Fig. 3B [see footnote 1]), the local 22% strain estimate can be extrapolated to the whole thrust domain, suggesting that the Tenerife thrust zone accommodates ~6.5 km of shortening. In comparison to a separate shortening calculation, regional bed length restorations of the Zapata–Punta Barrosa Formations in Figure 3B (see footnote 1) account for a comparable ~6.1 km magnitude of shortening across the Tenerife thrust domain.

Although the basal detachment in the Tenerife fault zone is parallel to bedding in outcrop, both the deformed stratigraphic section and fault zone have undergone subsequent open folding and form a regional fold, the Rio Rincón anti-

cline (Figs. 3 [see footnote 1] and 8B) (Wilson, 1983). This younger phase of folding uplifted and exposes volcanoclastic strata and hypabyssal intrusions of the Tobífera Formation, exposed within the core of Rio Rincón anticline (Fig. 3A [see footnote 1]), and is described in a subsequent section.

## Zircon U/Pb Age Constraints on Tenerife Thrusting

In order to constrain the maximum age of deformation in the Tenerife thrust domain, we dated a sample collected from a subhorizontal and undeformed gabbro sill that crosscuts tightly folded Punta Barrosa turbidite beds near the Torres del Paine granitic massif (Fig. 3A [see footnote 1]). This sample yields a zircon U/Pb age of  $16.9 \pm 0.2$  Ma (sample 07–72) (Fig. 7) and indicates that Tenerife thrust faulting and folding within the Upper Cretaceous Magallanes foreland basin occurred before this time.

## Rio Rincón–Castillo Thrusts

The surface exposure of the sub-Andean thrust belt in the Cordillera Arturo Prat (Fig. 3A [see footnote 1]), here named the Rio Rincón–Castillo thrust domain, is characterized by open folds in the Upper Cretaceous foreland basin strata, uplift of the Tobífera subvolcanic units, and localized thrust faults with tens of meters of offset. Wilson (1991) attributed this deformation to ramp-flat transitions of thrust faults at depth, indicative of thin-skinned shortening within the basin fill. However, subsurface imaging reveals that in addition to deformation within foreland strata, the regional structure of the Rio Rincón–Castillo thrust domain is predominantly influenced by basement structures (Fig. 3B [see footnote 1]). Seismic-reflection data from line ENAP-5004 show west-dipping, high-amplitude reflectors beneath the eastern flanks of Cerro Castillo that flatten with depth at 3 s two-way traveltime (TWTT) (Fig. 5). These structures are interpreted as deep-seated thrust faults that sole out in Paleozoic metamorphic basement complexes (e.g., Harambour, 2002). Displacement along the Rio Rincón and Castillo thrusts produces broad anticlines and synclines in the overlying Jurassic and Cretaceous basin fill (Fig. 3B [see footnote 1]).

The Rio Rincón anticline is one of the principal structures in the Patagonian thrust belt and consists of an extensive outcrop belt of uplifted and folded Zapata and Punta Barrosa Formations (Fig. 9B). The east-verging, asymmetrical Rio Rincón anticline (Figs. 3 [see footnote 1] and 8B) is cored by the Jurassic Tobífera Formation (Wilson, 1983), resulting in the easternmost surface exposure of preforeland basin basement

(Fig. 3 [see footnote 1]). There is no evidence for detachment of the Zapata Formation from the underlying volcanoclastic substrate; instead, the undisturbed depositional contact suggests that folding within both units is related to a deeper fault. Based on our extrapolation from nearby seismic-reflection data, ~10 km east (Fig. 3B [see footnote 1]), we propose that folding of the Tobífera Formation and Paleozoic basement is the result of displacement along the thrust fault ramp of a basement-seated thrust fault (Fig. 3B [see footnote 1]). Alternatively, the detachment level could reside atop the Paleozoic basement, but we prefer the former interpretation given that basement is uplifted and folded along imaged faults beneath Cerro Castillo (Fig. 3A [see footnote 1]).

Shortening across the Rio Rincón–Castillo basement thrust domain was estimated by restoring folded bed lengths and fault offsets in the Tobífera Formation. Seismic-reflection imaging of the Castillo basement thrusts aided this restoration and provided the basis for assuming a detachment depth beneath the Rio Rincón thrust fault (Fig. 3B [see footnote 1]). Our palinspastic restoration indicates ~3.4 km of shortening and almost 2 km of uplift of the Jurassic and Paleozoic basement beneath the foreland region. This magnitude of uplift is attributed to the deep-level detachment of the Castillo thrust, which soles out at ~8 km depth in the Paleozoic metamorphic basement (Fig. 3B [see footnote 1]). This detachment level is well-imaged in seismic-reflection data (Fig. 5), and we extend this interpretation westward beneath the Rio Rincón anticline (Fig. 8). However, an alternative geometry that should be considered is that the Rio Rincón fault instead soles out at the deeper, ~12 km detachment level, which would potentially result in a wider domain of deformation and presumably more basement shortening.

## Toro Thrust

The frontal outcrop belt of Upper Cretaceous–Neogene basin fill nearly parallels the Chile–Argentina border and forms the forelimb of the Toro anticline, named by ENAP geologists (Fig. 3A [see footnote 1]). At depth, 2-D seismic-reflection data from line ENAP-5004 capture the geometry of this frontal fold (Fig. 5). The Toro anticline is defined by uplifted and folded, high-amplitude reflectors that are draped by lower-amplitude, parallel reflectors (Fig. 5). Drill-core data from Toro-1B well indicate that this high-amplitude interval corresponds to Tobífera volcanoclastic rocks, which are overlain by shale of the Zapata Formation (Tower et al., 1980; Wilson, 1991). The Toro anticline is cored by westward-dipping, high-amplitude reflectors

in seismic-reflection data that are interpreted as a basement-seated thrust fault that soles out at nearly 5 s TWTT within the Paleozoic metamorphic basement (Figs. 3B [see footnote 1] and 5) (Harambour, 2002).

Reverse displacement along this structure culminates in a broad zone of deformation at the leading edge of the fault, and it accounts for uplift and folding of the Paleozoic basement, overlying Tobífera Formation, and Upper Cretaceous foreland strata. Shortening across the Toro anticline is partially accommodated by reactivation of Jurassic normal faults, thereby inverting an extensional graben as a later stage pop-up block along the leading edge of the Toro thrust (Fig. 5) (e.g., Buchanan and McClay, 1991). Palinspastic restoration of the Toro anticline by removing fault displacement and folding of the Tobífera Formation yields ~2.2 km of shortening. Most of the deformation associated with the Toro thrusting is expressed by nearly 5 km of basement uplift and broad folding of the Tobífera and Cretaceous–Paleogene foreland basin strata (Fig. 3B [see footnote 1]).

#### **Zircon U/Pb Constraints on the Timing of Toro Thrusting**

The timing of crustal shortening across the Toro anticline is best constrained by a deformed early Miocene gabbroic sill (sample 09–209) that intruded along horizontal layering within the Upper Cretaceous Tres Pasos Formation. Subsequent folding and eastward tilting of the section above the Toro thrust postdated the intrusion of the gabbro, which yields a zircon U/Pb age of  $20.6 \pm 0.4$  Ma (Figs. 3A [see footnote 1] and 7). Here, both shale beds and the gabbroic sill dip  $30^\circ$  east.

An additional estimate on the duration of Toro thrusting is indirectly provided by zircon U/Pb geochronology from the early Miocene synorogenic basin fill (Figs. 4 and 9C). This stratigraphic section displays growth strata that reflect progressive synsedimentary tilting related to thrust front advancement into the foreland basin (Fig. 3B [see footnote 1]) (e.g., DeCelles and Giles, 1996). Volcanic ash from the nonmarine Rio Guillermo Formation (09–237A) yields a zircon U/Pb age of  $21.7 \pm 0.3$  Ma (Figs. 3A [see footnote 1] and 7). The early Miocene ages from these samples (Figs. 3 [see footnote 1] and 4) are consistent with recent correlations by Parras et al. (2008) for the Paleogene–Neogene boundary in southern Patagonia. These results are also consistent with a period of Miocene explosive volcanism documented in subsurface ash layers of the El Salto Formation, ~200 km east of the batholith (Hervé et al., 2004; Casanova, 2005).

A second sample from this section, a dacite lava flow (09–226) from interbedded sandstone,

siltstone, and basalt flows in the Sierra de Los Baguales, yields a  $19.6 \pm 0.4$  Ma zircon U/Pb age (Figs. 3 [see footnote 1] and 7). This unit was previously grouped into the generalized Rio Bandurrias Formation (Wilson, 1983) and likely correlates to the Rio Guillermo Formation in the Santa Cruz Province (Fig. 3A [see footnote 1]) (Malumián and Caramés, 1997).

At the top of the Miocene sedimentary succession, volcanic ash was collected from the Santa Cruz Formation on Cordillera Chica (Figs. 3A [see footnote 1] and 4), where subhorizontal fluvial conglomerate and sandstone are overlain by Quaternary gravels (Fig. 3B [see footnote 1]). Sample 09–235A yields a zircon U/Pb age of  $18.1 \pm 0.4$  Ma (Fig. 7), consistent with  $^{40}\text{Ar}/^{39}\text{Ar}$  dating from the same formation farther north (Blisniuk et al., 2005). Together, these three volcanic zircon samples indicate that uplift and progressive tilting of the basin fill occurred between 22 and 18 Ma (Fig. 4). We attribute this syndepositional deformation to the growth of a monoclinical fold into the foreland associated with reverse-sense displacement along the underlying, deep-seated Toro thrust fault (Fig. 3B [see footnote 1]).

#### **SUBSURFACE STRATIGRAPHY OF THE MAGALLANES BASIN**

Seismic-reflection line YPF-AS8 depicts a 100-km-wide E-W cross-sectional view of the uplifted Cretaceous–Tertiary foreland basin fill and underlying attenuated basement (Fig. 6). In this section, we describe a sequence of stratigraphic intervals based on reflector geometry and visible offsets along interpreted faults. Correlations to the outcrop stratigraphy are relatively straightforward where stratigraphic intervals are uplifted and eroded. In other instances, we broadly correlate the subsurface intervals to our stratigraphic section in Figure 4 based on YPF–S.A. age determinations in well YPF-SC-1 and guided by the regional study by Biddle et al. (1986). The most prominent set of reflectors (interval A) in this line correlates to the Jurassic Tobífera Formation (Fig. 4), which fills rift grabens with up to 0.50 s TWTT of synrift volcanic and volcanoclastic deposits (Fig. 6). The Tobífera Formation unconformably overlies the extended Paleozoic basement (e.g., Chernikoff and Caminos, 1996; Pankhurst et al., 2003), which is characterized by chaotic reflectors with vague localized subhorizontal layering. In the larger structurally partitioned basins, reflectors exhibit a fanning geometry with increasing dip down-section toward normal faults (Fig. 6), indicative of syntectonic sedimentation. On the west side of the line, rift grabens are inverted, resulting in broadly folded reflectors (Fig. 6).

High-amplitude, discontinuous, and normal-faulted reflectors in interval A transition upward into laterally continuous and parallel reflectors that extend across the entire profile (interval B). Across rift grabens, reflectors exhibit a concave-up, parallel geometry that is interpreted as the result of postrift thermal subsidence and compaction (Fig. 6). Interval B is interpreted to correspond to the shale and siltstone of the Lower Cretaceous Zapata Formation in the Ultima Esperanza District (Fig. 4) (Fildani and Hessler, 2005) and the Lower Inoceramus Formation located farther east in Argentina (Biddle et al., 1986).

In the eastern region of the seismic-reflection line, interval B is overlain by sigmoidal reflectors that downlap onto the underlying strata (Fig. 6). We interpret the reflectors within this interval C as westward-prograding clinoforms that represent the muddy outer shelf and slope of the Early Cretaceous Rocas Verdes Basin (Figs. 4 and 6). This stratigraphic interval likely corresponds to the Upper Inoceramus Formation (pre–mid-Aptian) (Biddle et al., 1986, and references therein). We estimated the depth to the basin plain by measuring a 0.30 s TWTT interval between the bottom and top of these clinoforms. Using a standard velocity conversion of 2.5 km/s, the base of slope was at least 375 m below the shelf during Early Cretaceous time.

A regional foreland unconformity separates the Lower Cretaceous section (intervals B and C) from the overlying stratigraphic interval, which is characterized by low-amplitude reflectors with moderate eastward dip. These reflectors flatten toward the east, where they terminate in an onlap relationship (Fig. 6). This package, interval D, is generally conformable and contains small offsets and minor internal folding that are attributed to subsequent deformation (Fig. 6). The strongly asymmetric geometry and onlapping reflectors are interpreted as the clastic deposits that accumulated in a rapidly subsiding foreland basin. Stratigraphic age datum “ $K_{\text{top}}$ ” from well YPF-SC-1 indicates the location of the top of the Cretaceous basin fill (Fig. 5); therefore, we categorize the thick (~2.0 s) asymmetric interval D as the Upper Cretaceous fill of the Magallanes Basin (Fig. 4) (Romans et al., 2011).

In the western portion of the basin, the foreland basin fill contains a subtle angular unconformity that separates the more steeply dipping Upper Cretaceous interval from the overlying reflectors (Fig. 6). We correlate this surface to the outcrop unconformity between the Maastrichtian–Danian Dorotea Formation and the Eocene Rio Turbio Formation (Figs. 3 [see footnote 1] and 4) (Malumián and Caramés, 1997).

The angularity of this unconformity decreases eastward into the basin, where stratigraphic separation is minimal, and the Paleocene foreland basin fill is conformable with the underlying stratigraphic interval (Fig. 6).

Above the Paleocene unconformity, the Tertiary basin fill (interval E) is characterized by an interval of bright-amplitude, parallel, and continuous reflectors (Fig. 6). Based on stratigraphic age datum “Eoc<sub>a</sub>” from well YPF-SC-1 and correlations to the uplifted sections in outcrop (Figs. 3 [see footnote 1] and 4), this interval is interpreted as the sandstone and coal-rich Eocene Rio Turbio–Guillermo Formation and Oligocene–early Miocene Rio Leona Formation (Fig. 4) (Malumián and Caramés, 1997). The overlying reflectors (interval F) exhibit low amplitudes and an east-dipping, sigmoidal geometry with down-lapping terminations, likely representing the eastward-prograding Oligocene foreland basin fill (Figs. 4 and 6). These results document the change from N-S sedimentary transport in the Cretaceous basin to eastward transport of nonmarine sediments, consistent with the findings from other subsurface analyses of the Paleogene foreland basin fill (Biddle et al., 1986; Galeazzi, 1998), and foreland fill patterns in general.

Interval G, the highest stratigraphic package imaged in line YPF-as8 consists of high-amplitude, parallel reflectors that dip gently and flatten out toward the east (Fig. 6). The lower surface of this interval is moderately irregular and is interpreted as an erosional unconformity on the western side of the basin. This interval includes a stratigraphic age datum “Mio<sub>a</sub>” from well YPF-SC-1 that indicates an uppermost Lower Miocene age.

### Santa Cruz Thrust

Deformation along the western edge of the Magallanes basin involves broad folding of the basin fill and underlying Tobífera and Paleozoic rocks. This regional eastward tilting alludes to the presence of a fault at depth, thereby extending the zone of foreland thrust advancement into the basin nearly 30 km farther east than previously documented (Figs. 3B [see footnote 1] and 6). Although seismic-reflection data do not extend deep enough to resolve a structure in adequate detail (Fig. 6), seismic-reflection line ENAP-5004 depicts a deep detachment level associated with the Toro thrust (Fig. 5) (Hambour, 2002). As such, we suggest that a foreland fault, informally named the “Santa Cruz fault,” extends eastward from this detachment and accounts for tilting of the basin. Within the Paleogene basin fill above this fault zone, low-angle detachment faults result in shallow folding and

localized thickening of the overlying strata (Fig. 6). Localized faulting and minor folding are evident in the basin fill, including Miocene sedimentary rocks, indicating that thrust faulting occurred after their deposition.

### KINEMATIC EVOLUTION OF THE PATAGONIAN FOLD-AND-THRUST BELT

The structural and subsurface stratigraphic data presented here provide the foundation for a regional balanced cross section (Fig. 3B [see footnote 1]) and represent present-day boundary conditions for our kinematic reconstruction of the Patagonian fold-and-thrust belt in Figure 10. The sequential evolution of the thrust belt and its cogenetic foreland basin is evaluated using restored fault displacement, modeling of fold geometry, subsurface data, and geochronology (Fig. 3B [see footnote 1]). Additional constraints are drawn from detrital provenance records (Fildani et al., 2003; Sánchez, 2006; Romans et al., 2009b), low-temperature thermochronology (Thomson et al., 2001; Fosdick, 2008), and estimates of paleo-sea level from synorogenic basin fill (Malumián et al., 1999, 2001). We based our pin line (cf. Dahlstrom, 1969) in the undeformed foreland basin that is constrained by subsurface data (Fig. 3B [see footnote 1]). The magnitude of shortening for each stage was calculated across the retrodeformed distance between the Sarmiento ophiolitic complex and the leading edge of the thrust front beneath Cordillera Chica (Fig. 10).

#### Stage I: Onset of Retroarc Shortening

Regional convergence in the hinterland was under way by the end of the Early Cretaceous—the Rocas Verdes backarc basin had already been closed and its mafic crust had begun to shorten and obduct onto the South American margin (Fig. 10A) (Suárez and Pettigrew, 1976; Dalziel, 1981; Wilson, 1991; Fildani and Hessler, 2005; Calderón et al., 2007a). In this sector of the Patagonian Andes, the oldest phase of Andean contractional deformation is resolved by inferences from the stratigraphic record; understanding the details of initial thrusting is inhibited by lack of direct evidence for Cretaceous deformation along preserved structures. Additional complication arises from the possibility of reactivation of hinterland structures during later deformation.

The timing of tectonic basin inversion near 51°S is best understood from zircon U/Pb geochronology of the Upper Cretaceous basin fill. Previously, Fildani et al. (2003) documented the initiation of Magallanes Basin sedimenta-

tion ca. 92 Ma, using the youngest population of detrital zircons in the lowermost Punta Barrosa Formation. The predominance of thick (>1 m) turbidite sand beds reflects the presence of a well-developed fold-and-thrust belt by this time (Fildani and Hessler, 2005). In light of new U/Pb geochronology of volcanic ash (Fig. 7) interbedded with thin-bedded turbiditic sandstone and shale within the upper parts of the Zapata–Punta Barrosa “transition,” incipient thrust belt formation was under way as early as 101 Ma (Fig. 10A). Sandstone petrography, detrital zircon geochronology, and mudstone geochemistry indicate that sediment was derived from uplifted Paleozoic metamorphic basement complexes, the Sarmiento ophiolitic complex, and a juvenile volcanic arc (Fig. 10A) (Fildani and Hessler, 2005).

The Canal de las Montañas shear zone is a likely candidate for the early thrusting in the hinterland that was responsible for basin flexure during Punta Barrosa deposition (Fig. 3A [see footnote 1]). Zircon U/Pb data from an undeformed granodiorite within the Sarmiento ophiolitic complex, west of the Canal de las Montañas shear zone, indicate pluton emplacement ca. 80 Ma. These findings constrain the locus of arc magmatism during this time interval and suggest that the main deformation along the Canal de las Montañas shear zone occurred prior to 80 Ma (Calderón et al., 2009). Other candidate structures that were active as early as 100 Ma have not been identified.

#### Stage II: Tobífera Duplex Growth and Thrusting

During Coniacian time, retroforeland convergence resulted in shortening within the volcanic-volcaniclastic Tobífera Formation, and formation of an imbricate thrust or antiformal stack that appears to have involved attenuated Paleozoic basement (Fig. 10B). Our preferred palinspastic reconstruction of this shortening is based on modeled fold geometry of antiformal thrust sheets that sole out atop the Paleozoic basement, accommodating ~27 km of shortening (~16%). A more conservative estimate using a stacked thrust sheet geometry accounts for ~20 km of shortening. We prefer the former interpretation (Fig. 10B) because it is corroborated by existing *P-T* estimates of syntectonic metamorphism for the Tobífera tectonic burial to depths of ~15–20 km between 150 and 100 Ma (Galaz et al., 2005; Calderón et al., 2007a; Hervé et al., 2007b). Secondly, the substantial basin deflection recorded by >2000 m paleobathymetry of the Cerro Toro Formation alludes to a substantial topographic load in the fold-and-thrust belt, which is easily accommodated by a

stacked, antiformal duplex structural geometry. Accounting for uncertainties in the structure, we conservatively postulate that between ~20 and 27 km of shortening (12%–16%) was taken up across the Tobífera thrusts (Fig. 10B).

While thrusting along specific structures is difficult to identify in the Tobífera duplex, enhanced regional exhumation is suggested by K-Ar cooling ages from the Sarmiento ophiolitic complex that cluster around 74 Ma (Rapalini et al., 2008), supporting rapidly eroding, thickened crust at this time. Additional timing constraints on Tobífera thrusting come from the detrital provenance signature of the foredeep basin fill: The Cerro Toro Formation records the appearance of Upper Jurassic zircons beginning ca. 88 Ma (Romans et al., 2009b) and Tobífera rhyolitic clasts (Sánchez, 2006; Crane and Lowe, 2008) and indicates unroofing of Tobífera thrust sheets by Coniacian time. Topographic growth of the Tobífera duplex at this time is consistent with enhanced foredeep flexural subsidence and deposition of the shale-rich Cerro Toro Formation in water depths greater than 2000 m (Natland et al., 1974). By 80 Ma, the Sarmiento and Tobífera rocks were intruded by isolated epizonal plutons of Campanian age (Calderón et al., 2009), indicating an eastward shift in the locus of arc magmatism and foreland deformation. In light of these various temporal constraints, we propose that substantial exhumation and inferred deformation of the Tobífera duplex occurred between 88 and 74 Ma (Fig. 10B).

During stage II deformation, synsedimentary thrust faults and/or reactivation of Jurassic rifts appear to have localized axial submarine drainage in the Magallanes foredeep (Fig. 3B [see footnote 1]). An assessment of the axial channel stratigraphy (Winn and Dott, 1979; Hubbard et al., 2008) combined with subsurface data shows a remarkable spatial correlation between the location of the basin axis and the directly underlying Jurassic extensional graben in the Paleozoic basement (Figs. 5 and 10B). In particular, the Late Jurassic graben developed in Paleozoic basement beneath Cerro Castillo (Fig. 6) and the main channel axis of the deep-water Cerro Toro Formation (Figs. 3 [see footnote 1] and 5) (Hubbard et al., 2008) and demonstrates a long-standing spatial localization of an axial sediment dispersal pattern (Bernhardt et al., 2011).

### **Stage III: Campanian–Early Oligocene Tenerife Thrusting**

Stage III deformation is characterized by faulting and folding of the Zapata, Punta Barrosa, and Cerro Toro Formations in the Tenerife thrust zone (Fig. 10C). During this stage of

shortening, the Andean thrust front advanced ~30 km into the foreland along an inferred Paleozoic detachment, and the higher-level Tenerife thrust zone (Fig. 9B) developed between the Zapata and Punta Barrosa Formations (Fig. 3B [see footnote 1]). Palinspastic reconstructions of deformation indicate ~6.1 km of shortening (4%) across the Tenerife thrust domain (Fig. 10C). Tight folding and faulting of the Punta Barrosa Formation are localized in the hanging walls of thrust faults (Fig. 8C).

Farther east in the hinterland, paleomagnetic data suggest ~30° counterclockwise horizontal-axis rotation of the Sarmiento ophiolitic complex, which has been attributed to thrusting and fault rotation, possibly along inverted Mesozoic normal faults (Rapalini et al., 2008). Although the timing of rotation is only constrained to postdate magnetic remanence acquisition in Late Cretaceous time, ca. 75–72 Ma (Rapalini et al., 2008), for geologic simplicity we account for this deformation in stage III Tenerife thrusting. Rotation could alternatively have been associated with a younger phase(s) of deformation. In our simplified model, east-vergent thrusting is expressed by out-of-sequence faulting in the Sarmiento ophiolitic complex and Tobífera thrusts along mapped high-angle shear zones (Fig. 10C) (Calderón et al., 2005, 2009; Galaz et al., 2005).

Thin-skinned deformation across the Tenerife thrust sheet is only loosely constrained by the available data, and this leads to higher uncertainties in shortening rates during Tenerife thrusting. While acknowledging this ambiguity, we can evaluate the general sense of timing using stratigraphic principles and crosscutting relationships. We infer that deformation began at least after deposition of the 87–82 Ma Cerro Toro Formation (Kct), which was involved in thrusting and is preserved in outcrop as far west as Cerro Donoso and Cerro Ferrier atop the Tenerife thrust sheet (Fildani and Hessler, 2005). One of the faults within the Tenerife thrust zone, the Rio Nutria thrust, displaces Punta Barrosa Formation atop the Cerro Toro Formation (Fig. 3A), pointing to a post–Cerro Toro Formation age for Tenerife thrusting. The minimum age of deformation was evaluated by silicic intrusions that were emplaced along the Patagonian Andes, including Cerro Balmaceda, Cerro Donoso, Torres del Paine, and Cerro Fitz Roy (Michael, 1983; Michel et al., 2008; Sánchez et al., 2008). In the study area, the thin-skinned structures of the Tenerife thrust sheet are intruded by the 27 Ma Cerro Donoso granite (Sánchez et al., 2008), which crosscuts deformed shale and sandstone beds in the Zapata and Punta Barrosa Formations and provides a minimum age of deformation (Figs. 3 [see footnote 1] and 7).

The presence of the ~15 m.y. unconformity within the Paleocene basin fill, followed by resumed deposition of an eastward-building progradational shallow-marine foreland system during Eocene–Oligocene time (Malumíán et al., 1999, 2001), alludes to significant uplift of the retroforeland region. We postulate that internal deformation associated with Tenerife thrusting caused this foreland uplift and erosion, thereby using the depositional history to better resolve when Tenerife thrusting occurred during the ca. 74–27 Ma time period (Fig. 10C).

Additional insight into Paleogene foreland paleogeography is provided by the Eocene–Oligocene deltaic and lagoonal Rio Turbio Formation (Figs. 3A [see footnote 1] and 4), which indicates that sedimentation at this location was near sea level at ca. 33 Ma. We extrapolate this sea-level datum toward the hinterland to estimate the location of the Paleogene frontal thrust, likely located at the leading edge of the Tenerife thrust sheets. Palinspastic restoration of stage III thrusting accounts for ~6.1 km of shortening (Fig. 10C), resulting in a paleogeographic reconstruction of a substantial mountain range, ~60 km wide, that potentially isolated the shallow-marine and deltaic foreland depocenter from eastward transport of magmatic detritus, a relationship common in retroforeland systems (e.g., Dickinson, 1976).

### **Stage IV: Late Oligocene–Early Miocene Rio Rincón–Castillo Thrusting**

Early Oligocene–early Miocene deformation of the Rio Rincón–Castillo basement thrust domain accounts for ~3.4 km of shortening (2%) and nearly 2 km of uplift in the Jurassic and Paleozoic basement (Fig. 10D). This magnitude of uplift and thrust advancement into the foreland was probably associated with substantial topographic growth of the fold-and-thrust belt. Foreland deposition of the Rio Turbio Formation at this time is characterized by eastward-prograding shallow-marine systems (Fig. 6) (Malumíán et al., 2001), indicating an important change from southward, axial sediment dispersal patterns consistently indicated by the deep-water formations (e.g., Romans et al., 2011), to a dominantly orthogonal paleo-drainage network off of the thrust front. This paleogeographic depiction is consistent with zircon (U-Th)/He thermochronologic cooling ages from the Tobífera Formation in the Rio Rincón anticline (Fig. 3B). These data suggest that ~6–7 km of overburden once covered the area until 20 Ma (Fosdick, 2008), which may reflect substantial structural topography within the Rio Rincón thrust block in early Miocene time. Figure 10C shows the estimated location

of a ca. 20 Ma surface above the Tobífera Formation in Rio Rincón. Together with the paleotopographic estimates from the Rio Rincón thrust block, this suggests that the Rio Rincón anticline may have been the frontal thrust into the Paleogene foreland basin (Fig. 10D).

### Stage V: Early Miocene Toro Thrusting

Deformation within the Toro thrust domain accounts for uplift and broad folding of the Paleozoic basement through Danian basin fill (Figs. 2 and 10E). A factor of particular significance is the substantial deepening of the basal detachment of the Toro thrust, which soles out at nearly 15 km depth (Fig. 10E), likely along a zone of weakness in the Paleozoic basement. This structure is well imaged in seismic-reflection data (Fig. 5) and implies a change in orogenic dynamics that promoted thrusting along a deeper detachment, giving rise to a broad zone of uplift and relatively less shortening (Fig. 10E). Crustal shortening across both the Rio Rincón–Castillo and Toro thrust domains implies basement detachments, and the detachment level of the Toro thrust (~9 km) is significantly deeper than that of the Rio Rincón–Castillo faults (~4 km depth) (Fig. 5), indicating multiple levels of detachment surfaces within Paleozoic basement. Drill cores of the Tierra del Fuego basement show shallowly dipping foliated gneisses, consistent with existence of subhorizontal detachment levels (Forsythe, 1982; Galeazzi, 1998).

In this kinematic reconstruction, we use the early Miocene Rio Guillermo deltaic margin as an approximate sea-level datum for restoring tilting of the Paleogene synorogenic basin fill (Fig. 10E). Palinspastic restoration of shortening during stage V deformation yields ~2.2 km of shortening (1.4%) and uplift of the Jurassic and Paleozoic basement. This deformation occurred between 21 and 18 Ma and was synchronous with early Miocene sedimentation until 18 Ma, when deposition of fluvial deposits blanketed the foreland (Malumián and Caramés, 1997; Malumián et al., 1999, 2001; Blisniuk et al., 2005).

### Stage VI: Post-18 Ma Regional Uplift and Exhumation

Stage VI deformation includes Santa Cruz thrusting and uplift of the Neogene basin (Fig. 10F). The timing of this deformation is poorly constrained but likely postdates deposition of the Santa Cruz Formation, ca. 18 Ma (Fig. 4), and may have been coeval with subduction of the Chile Ridge (Ramos and Kay, 1992; Goring et al., 1997; Ramos, 2005). In an effort

to evaluate the effects of long-wavelength regional uplift from the late-stage thrust-related shortening, we restored tilting on the middle Miocene (post-ridge collision) strata within the basin and applied this regional tilt correction to the thrust belt (Fig. 10F). In this manner, we can approximate the results of Neogene uplift across Patagonia, possibly related to dynamic processes associated with ridge subduction (Guillaume et al., 2009), in our final stage of reconstruction. The resulting ~4 km of uplift that we restore between pre-stage IV and present-day configuration is consistent with estimates of exhumation magnitude in late Miocene time (Fosdick, 2008).

## DISCUSSION

### Magnitude and Timing of Deformation

Our palinspastic reconstructions of the Patagonian fold-and-thrust belt indicate ~12 km (7%) of shortening within the Cretaceous–Tertiary foreland basin following closure of the Rocas Verdes Basin and initial foreland compression (Fig. 10). An additional 20–27 km (12%–16%) is postulated for the Tobífera duplex (Fig. 10B), although uncertainties in the internal structure of the Cordillera de los Andes preclude a precise constraint on shortening. Given the lack of subsurface data from the western part of the study area, i.e., the Tobífera and Tenerife thrust domains (Fig. 3A), we view the structural reconstructions with considerable uncertainty in this area and consider our range to represent two extreme geometries. Accounting for these uncertainties, our results illustrate a moderately shortened foreland (32–40 km or 19%–23%), where the overall magnitude of shortening appears to decrease over time, preserving the uppermost Cretaceous through Neogene foreland basin deposits within thrust sheets that have undergone little transport (Fig. 3B). Instead, the vertical component of foreland deformation noticeably increases during early Oligocene–early Miocene thrusting, which we attribute to the reverse displacement along deeper thrust faults rooted in the Paleozoic basement complexes.

The minimum estimates of regional shortening across the whole retroforeland fold-and-thrust belt, excluding Rocas Verdes Basin closure and underthrusting, are comparable with those calculated from the fold-and-thrust belt north of our study area near 50°S (Ramos, 1989; Kraemer, 1998). In this northern segment, roughly at the limit of Rocas Verdes Basin quasi-oceanic crust (Fig. 1), Kraemer (1998) documented 35 km (26%) of shortening that accrued during Eocene and Miocene episodes.

Although our shortening estimates are comparable, though slightly less, a significant difference in the 51°30'S transect is that our analysis documents a significant contribution from Late Cretaceous deformation (Fig. 10). Previous workers have observed a pronounced distributed strain gradient along the Patagonian orocline (e.g., Ghiglione and Cristallini, 2007), from less than 10–25 km of shortening near Lago Argentino (Ramos, 1989; Coutand et al., 1999) to ~100 km (Klepeis et al., 2010) and perhaps up to ~170 km of orogenic shortening accommodated in the Fuegian fold-and-thrust belt (Fig. 1) (Winslow, 1982; Klepeis, 1994; Ghiglione and Ramos, 2005; Kraemer, 2003).

In Tierra del Fuego, the magnitude of shortening appears to be equivalent across the hinterland and foreland, where ~50 km is documented in the Cordillera Darwin (Klepeis et al., 2010), and an additional 50 km of foreland shortening is reported above the Tobífera Formation (Rojas and Mpodozis, 2006). In contrast, our results suggest that instead of a 1:1 ratio of hinterland and foreland deformation, shortening across the Tobífera duplex is more than twice the amount documented in the Late Cretaceous–Neogene foreland basin fill. This observation may be accentuated by the effects of error propagation, in that the earlier stages of deformation are not as well-defined as subsequent foreland shortening.

Compression initiated at 51°30'S ca. 100 Ma, and a well-developed fold-and-thrust belt was present by 92 Ma (Fig. 10) (Fildani et al., 2003). The onset of compression in the Ultima Esperanza region was synchronous with the deformational history in Tierra del Fuego (Klepeis et al., 2010), suggesting along-strike continuity of subduction dynamics of the South American plate margin. The deepest phase of foreland subsidence and foredeep sedimentation (Cerro Toro Formation) occurred in the Coniacian–early Campanian (ca. 88–74 Ma) during structural thickening and exhumation of the Tobífera thrusts. Stage III Tenerife thick-skinned thrusting is broadly defined between ca. 74 and 27 Ma and overlapped in time with crustal shortening in the Fuegian foreland, ca. 56–34 Ma (Ghiglione and Ramos, 2005), ca. 39 Ma exhumation of the orogenic hinterland (Barbeau et al., 2009), and Paleogene internal thickening and exhumation of the Cordillera Darwin (Klepeis et al., 2010). Tenerife thrusting into the foreland probably represents widening of the orogenic wedge via thrust propagation sometime between ca. 74 and 27 Ma in response to topographic growth during Tobífera duplex formation. Although our estimates of precisely when Tenerife thrusts were active are limited by available age constraints, stratigraphic relationships in the foreland suggest that missing strata

from 60 to 45 Ma may be associated with a phase of deformation and uplift in the thrust belt (Wilson, 1991; Malumíán et al., 1999).

Cenozoic plate reorganization along the Patagonian margin has contributed to spatio-temporally variable deformation in the Andean orogen (Cande and Leslie, 1986; Gorrington et al., 1997; Suárez et al., 2000; Ghiglione and Ramos, 2005). The initiation of Rio Rincón–Castillo thrusting ca. 27 Ma (stage IV) coincided with the breakup of the Farallon plate ca. 26 Ma, and may have been caused by both increased and more trench-perpendicular convergence between the oceanic Nazca and South American plates (Lonsdale, 1995). Deposition of the Oligocene–Miocene synorogenic foreland basin fill has been linked to this change in subduction dynamics (Ramos, 1989; Malumíán et al., 2001) and likely reflects orogenic wedge growth and erosion in response to compressive stresses transmitted from the trench into the retroforeland.

An important phase of foreland deformation and uplift occurred ca. 21–18 Ma Toro thrusting (stage V), during which time over 800 m of (compacted) sediments accumulated during active arc volcanism (Fig. 4). This stage of deformation is well-constrained by geochronology of crosscutting intrusions and synorogenic Rio Guillermo and Santa Cruz Formations (Fig. 7) and predates Neogene subduction of the Chile Ridge (Cande and Leslie, 1986; Gorrington et al., 1997). Seismic-reflection data image the geometry of basement-seated thrust faults and suggest a shift in structural style to higher-angle basement thrusts that sole out near 12 km depth in the Paleozoic metamorphic basement.

This development of basement uplifts may have been a response to a stronger coupling between the continental and oceanic lithospheres during initial impingement of the Chile Ridge spreading system with the Patagonian margin (Cande and Leslie, 1986; Gorrington et al., 1997; Ramos, 2005). A recent kinematic reconstruction of the subducted ridge system beneath Patagonia suggests that the spreading center first began to enter the Chile Trench in Tierra del Fuego as early as 20 Ma (Breitsprecher and Thorkelson, 2009) and fully collided with Patagonia at the latitude of our study area by 16–14 Ma (Cande and Leslie, 1986; Gorrington et al., 1997; Breitsprecher and Thorkelson, 2009). We speculate that this change along the convergent margin caused increased foreland shortening in the Ultima Esperanza and Santa Cruz Province. As the Chile triple junction migrated north, basement structures such as the Santa Cruz thrust beneath the Magallanes foreland may have accommodated regional basement-seated uplift (Harambour, 2002). Given the spatial correlation between preexisting extensional

domains and subsequent thrust sheets, e.g., the Castillo, Toro, and Santa Cruz thrusts (Fig. 3), a rifted basement may have provided such a mechanism for accommodating internal deformation and late-stage thrust faulting.

### Effects of Attenuated Crust

The development of foreland convergence across attenuated Rocas Verdes Basin crust manifests several important characteristics that are important to collisional retroforeland basins. It has long been known that inherited extensional structures can exert a control on the broader deformational and sedimentation patterns during subsequent foreland convergence (Bond and McClay, 1995; Lowell, 1995). In this sense, the spacing and location of preexisting extensional domains correspond to the location where subsequent thrust faults form during compression (e.g., Kraemer, 1998; Harambour, 2002). The highly attenuated crust beneath the Magallanes retroforeland basin represents an end-member example where rifting progressed enough to form quasi-oceanic crust. Where we can characterize the subsurface structure of frontal thrusts into the Magallanes Basin, the spacing of both extensional domains and younger principal thrust sheets is between 40 and 30 km, namely, the Rio Rincón, Toro, and Santa Cruz thrusts (Fig. 6). The spatial coincidence of these domains suggests a control from the inherited extensional extended crust on the spacing of thrust sheets. In fact, the spacing appears to decrease systematically eastward into the foreland, perhaps as a function of encroachment of less attenuated and more widely spaced extensional domains (Fig. 3B). Such a relationship has important implications for rates of thrust front propagation (DeCelles and DeCelles, 2001), particularly in settings where inherited extensional strain is spatially variable. For instance, if extended zones of weakness are exploited as basement thrust ramps, increasing fault spacing could cause a corresponding increase in thrust front propagation rate.

Extensional strain gradients developed across marginal basins would similarly affect the subsequent foreland basin phase. Thinned lithosphere develops a reduced flexural rigidity, such that flexural basins that form in response to crustal loading are relatively narrower than their unextended counterparts (e.g., Flemings and Jordan, 1990; Desegaulx et al., 1991; Watts, 1992). This relationship is exemplified by the narrow fore-deep filled by deep-water (>1000 m) clastic sediments of the Magallanes Basin (Wilson, 1991; Fildani and Hessler, 2005; Romans et al., 2011). In the Magallanes foreland subsurface, reconstructions of rifted crust in seismic-reflection

data account for only 10% extension, which is accommodated by localized minibasins in the Paleozoic basement (Fig. 6). Crustal thickness also appears to decrease westward across this domain from normal continental thickness (36 km) to 28 km beneath the *thickened* thrust belt (Fig. 2) (Robertson et al., 2003; Lawrence and Wiens, 2004). The anomalously low present-day crustal thickness beneath the thrust belt (Fig. 2) suggests that a pre-shortened Rocas Verdes Basin constituted significantly thinner crust, which underwent foreland flexure and shortening during Andean orogenesis.

Although we cannot assess the magnitude of Late Jurassic extension in the Paleozoic basement beneath the present-day thrust belt, we can infer a significant extensional strain gradient increasing westward from the foreland over a (contractional) retrodeformed distance of ~160 km, judging by the moderately attenuated Paleozoic basement beneath the Magallanes Basin (Fig. 6) and presence of coeval Late Jurassic quasi-oceanic crust exposed in the Sarmiento ophiolitic complex (Fig. 10A). These constraints require the transition to quasi-oceanic crust across this opposing rifted margin to have been somewhat large, akin to the asymmetric eastern margin of the Iberia–Newfoundland conjugate margin system (e.g., Keen and de Voogd, 1988). Early stages of thrust loading in the Patagonian thrust belt were caused by obduction of the marginal basin fill and underlying quasi-oceanic crust onto the South American margin (Dalziel, 1981; Calderón et al., 2007a; Fildani and Hessler, 2005; Romans et al., 2009b). We infer that the highly attenuated (>50%) transitional crust has been since removed or accreted beneath the Sarmiento ophiolitic complex suture and the Patagonian fold-and-thrust belt developed on transitional and progressively less extended continental crust (Fig. 2).

### CONCLUSIONS

This study presents the kinematic evolution of the Patagonian fold-and-thrust belt and combines the genetically linked stratigraphic history of the Magallanes foreland basin to describe the time-transgressive patterns of orogenic deformation in collisional retroarc basins. Combined results from several integrated data sets suggest that the regional Jurassic extensional domains that developed in the Paleozoic metamorphic basement, 30–40 km apart, exert a control on the spatial location of fold-and-thrust belt deformational domains. The influence of inherited structures is evident in continental retroarc thrust belts with rifted passive margins (e.g., the Central Andes); however, circumstances in collisional retroforeland where oceanic crust is

involved appear to accentuate the role of inherited extensional structures.

We postulate that deformation at 51°30'S began ca. 100 Ma and progressed during six principal stages of foreland shortening following closure of the Rocas Verdes Basin. A palinspastic restoration based on outcrop and subsurface mapping of stratigraphy and major structures indicates that at least 32–40 km of retroforeland shortening was accommodated across the 160-km-wide thrust belt, representing ~19%–23% shortening. At least 12 km of shortening is documented across the Cretaceous basin fill, accompanied by ~5 km of uplift and exposure of preforeland rocks along basement-rooted thrust faults.

Uplift of basement blocks in the retroforeland corresponds to a deepening of the detachment level during middle Miocene time, resulting in vertical uplift of the fold-and-thrust belt, although this was accompanied by significantly less shortening. As a comparative example, basement-cored uplift provinces in the Sierras Pampeanas ranges in the Central Andes and the Cretaceous Laramide uplifts of the western United States are well understood in the context of flat-slab subduction (e.g., Dickinson and Snyder, 1978; Jordan and Allmendinger, 1986; Ramos et al., 2002). In contrast, the Patagonian Andes exhibit similar subsurface basement uplifts that formed in the absence of any documented flat-slab subduction. We speculate that the shift in structural style to basement uplifts reflects the combined results of (1) increased coupling between the continental and oceanic lithospheres as the Chile spreading ridge approached the South American plate margin ca. 20 Ma, and (2) foreland shortening across previously attenuated and structurally segmented continental basement.

#### ACKNOWLEDGMENTS

The authors acknowledge George Hilley, Peter DeCelles, Thomas Moore, Stephen Hubbard, Donald Lowe, and Lisandro Rojas for insightful discussions on thrust belts and foreland basin systems. We gratefully acknowledge Empresa Nacional del Petróleo-Sipetrol (ENAP-Sipetrol) and Repsol Yacimientos Petrolíferos Fiscales Sociedad Anónima (Repsol YPF) for permission to publish seismic-reflection data. Superb field support was provided by Lisa Stright, Kenneth Gillingham, Alessandro Airo, Jake Covault, Zane Jobe, Dominic Armitage, and the yacht *Morgane* crew. We thank Schlumberger (Petrel™) and Halliburton (LithoTect™) for academic software licenses. We thank the Stanford U.S.G.S. Micro Analysis Center (SUMAC) laboratory personnel for assistance with sample preparation and data collection and reduction. This project was funded by the Geological Society of America (GSA) Student Research Grant program, the A.I. Levorsen Fund, American Association of Petroleum Geologists (AAPG) Grant-in-Aid, the American Alpine Club, industry sponsors of SPODDS (Stan-

ford Project on Deep-Water Depositional Systems), and Fondecyt Grant 11075000 to Calderón. Special thanks are due to the Torres del Paine and Bernardo O'Higgins National Parks and to ranch owners Don Luis Guerrero and Don Miguel Angel for access to the study area. We thank Matthew Coble, Keith Klepeis, Associate Editor Robert Butler, and an anonymous reviewer for thorough reviews.

#### REFERENCES CITED

- Alabaster, T., and Storey, B.C., 1990, Modified Gulf of California model for South Georgia, north Scotia Ridge, and implications for the Rocas Verdes back-arc basin, southern Andes: *Geology*, v. 18, p. 497–500, doi: 10.1130/0091-7613(1990)018<0497:MGOCMF>2.3.CO;2.
- Allen, R.B., 1982, Geología de la Cordillera Sarmiento, Andes Patagónicos, entre los 50°00' y 52°15' Lat. S, Magallanes, Chile: Servicio Nacional de Geología y Minería, Chile, Boletín (Instituto de Estudios de Población y Desarrollo [Dominican Republic]), v. 38, p. 1–46.
- Alvarez-Marrón, J., McClay, K.R., Harambour, S., Rojas, L., and Skarmeta, J., 1993, Geometry and evolution of the frontal part of the Magallanes foreland thrust and fold belt (Vicuña area), Tierra del Fuego, southern Chile: *American Association of Petroleum Geologists Bulletin*, v. 77, p. 1904–1921.
- Armitage, D.A., Romans, B.W., Covault, J.A., and Graham, S.A., 2009, The influence of mass transport deposit surface topography on the evolution of turbidite architecture: The Sierra Contreras, Tres Pasos Formation (Cretaceous), southern Chile: *Journal of Sedimentary Research*, v. 79, p. 287–301, doi: 10.2110/jsr.2009.035.
- Barbeau, D.L., Olivero, E.B., Swanson-Hysell, N.L., Zahid, K.M., Murray, K.E., and Gehrels, G.E., 2009, Detrital-zircon geochronology of the eastern Magallanes foreland basin: Implications for Eocene kinematics of the northern Scotia Arc and Drake Passage: *Earth and Planetary Science Letters*, v. 20, p. 23–45.
- Beaumont, C., Fullsack, P., and Hamilton, J., 1992, Erosional control of active compressional orogens, in McClay, K.R., ed., *Thrust Tectonics*: London, Chapman and Hall, p. 1–18.
- Bernhardt, A., Jobe, Z.R., and Lowe, R., 2011, Stratigraphic evolution of a submarine channel lobe complex system in a narrow fairway within the Magallanes foreland basin, Cerro Toro Formation, southern Chile: *Marine and Petroleum Geology* (in press), doi: 10.1016/j.marpetgeo.2010.05.013.
- Biddle, K.T., Uliana, M.A., Mitchum, R.M., Jr., Fitzgerald, M.G., and Wright, R.C., 1986, The stratigraphic and structural evolution of the central and eastern Magallanes Basin, southern South America, in Allen, P.A., and Homewood, P., eds., *Foreland Basins*: International Association of Sedimentologists Special Publication 8, p. 41–61.
- Blatt, H., 1979, Diagenetic process in sandstones, in Schoole, P.A., and Schluger, P.R., eds., *Aspects of Diagenesis*: Society for Sedimentary Geology Special Publication 26, p. 141–157.
- Blisniuk, P.M., Stern, L.A., Chamberlain, C.P., Idelman, B., and Zeitler, P.K., 2005, Climate and ecological changes during Miocene surface uplift in the southern Patagonian Andes: *Earth and Planetary Science Letters*, v. 230, p. 125–142, doi: 10.1016/j.epsl.2004.11.015.
- Bond, R.M.G., and McClay, K.R., 1995, Inversion of a Lower Cretaceous extensional basin, south central Pyrenees, Spain, in Buchanan, J.G., and Buchanan, P.G., eds., *Basin Inversion*: Geological Society of London Special Publication 88, p. 415–431.
- Breitsprecher, K., and Thorkelson, D.J., 2009, Neogene kinematic evolution of the Nazca–Antarctic–Phoenix slab windows beneath Patagonia and the Antarctic Peninsula: *Tectonophysics*, v. 464, p. 10–20, doi: 10.1016/j.tecto.2008.02.013.
- Bruhn, R.L., and Dalziel, I.W.D., 1977, Destruction of the Early Cretaceous marginal basin in the Andes of Tierra del Fuego, in Talwani, M., and Pitman, W.C., III, eds., *Island Arcs, Deep Sea Trenches, and Back-Arc Basins*: American Geophysical Union, Maurice Ewing Series 1, p. 395–405.
- Buchanan, P.G., and McClay, K.R., 1991, Sandbox experiments of inverted listric and planar fault systems: *Tectonophysics*, v. 188, p. 97–115, doi: 10.1016/0040-1951(91)90317-L.
- Calderón, M., Fildani, A., Hervé, F., Fanning, C.M., Weislogel, A., and Cordani, U., 2007a, Late Jurassic bimodal magmatism in the northern sea-floor remnant of the Rocas Verdes Basin, southern Patagonian Andes: *Journal of the Geological Society of London*, v. 164, p. 1011–1022, doi: 10.1144/0016-76492006-102.
- Calderón, M., Hervé, F., Cordani, U., and Massonne, H.-J., 2007b, Crust-mantle interactions and generation of silicic melts: Insights from the Sarmiento Complex, southern Patagonian Andes: *Revista Geológica de Chile*, v. 43, no. 2, p. 249–275.
- Calderón, M., Fosdick, J., Alvarez, J., Sánchez, A., and Galaz, G., 2009, Doubly-vergent structures in metamorphic rocks that enclose the Sarmiento ophiolite complex at Senos Lotos and Encuentros, southern Patagonian Andes (51–52°S): *Congreso Geológico Chileno Proceedings*, p. S8–004.
- Cande, S.C., and Leslie, R.N., 1986, Late Cenozoic tectonics of the southern Chile Trench: *Journal of Geophysical Research*, v. 91, p. 471–496, doi: 10.1029/JB091iB01p00471.
- Casanova, P., 2005, Estudio Sedimentológico de los Principales Reservorios de la Formación El Salto, en el Área de Dorado Sur, Magallanes, Chile [MS thesis]: Universidad de Chile, 58 p.
- Celaya, M., and McCabe, R., 1987, Kinematic model for the opening of the Sea of Japan and the bending of the Japanese Islands: *Geology*, v. 15, p. 53–57, doi: 10.1130/0091-7613(1987)15<53:KMFTOO>2.0.CO;2.
- Chernikoff, C.J., and Caminos, R., 1996, Estructura y relaciones estratigráficas de la Formación Nahuel Niyeu, Macizo Norpatagónico oriental, Provincia de Río Negro: *Revista de la Asociación Geológica Argentina*, v. 51, p. 201–212.
- Christensen, N.I., and Mooney, W.D., 1995, Seismic velocity structure and composition of the continental crust: A global view: *Journal of Geophysical Research*, v. 100, p. 9761–9788, doi: 10.1029/95JB00259.
- Coutand, I., Diraison, M., Cobbold, P.R., Gapais, D., Rossello, E.A., and Miller, M., 1999, Structure and kinematics of a foothills transect, Lago Viedma, southern Andes (49°30'S): *Journal of South American Earth Sciences*, v. 12, p. 1–15, doi: 10.1016/S0895-9811(99)00002-4.
- Covault, J.A., Romans, B.W., and Graham, S.A., 2009, Outcrop expression of a continental-margin-scale shelf-edge delta from the Cretaceous Magallanes Basin, Chile: *Journal of Sedimentary Research*, v. 79, p. 523–539, doi: 10.2110/jsr.2009.053.
- Crane, W.H., and Lowe, D.R., 2008, Architecture and evolution of the Paine channel complex, Cerro Toro Formation (Upper Cretaceous), Silla syncline, Magallanes Basin, Chile: *Sedimentology*, v. 55, p. 979–1009, doi: 10.1111/j.1365-3091.2007.00933.x.
- Dahlen, F.A., 1990, Critical taper model of fold-and-thrust belts and accretionary wedges: *Annual Review of Earth and Planetary Sciences*, v. 18, p. 55–99, doi: 10.1146/annurev.earth.18.050190.000415.
- Dahlstrom, C.D.A., 1969, Balanced cross sections: *Canadian Journal of Earth Sciences*, v. 6, p. 743–757.
- Dalziel, I.W.D., 1981, Back-arc extension in the southern Andes: A review and critical reappraisal: *Royal Society of London Philosophical Transactions*, v. 300, p. 319–335.
- Dalziel, I.W.D., 1986, Collision and cordilleran orogenesis: An Andean perspective, in Coward, M.P., and Ries, A.C., eds., *Collision Tectonics*: Geological Society of London Special Publication 19, p. 389–404.
- Dalziel, I.W.D., and Cortés, R., 1972, Tectonic style of the southernmost Andes and the Antarctic: *Montreal, Canada, International Geological Congress Proceedings*, v. 3, p. 316–327.
- Dalziel, I.W.D., de Wit, M.J., and Palmer, K.F., 1974, Fossil marginal basin in the southern Andes: *Nature*, v. 250, p. 291–294, doi: 10.1038/250291a0.
- Davis, D., Suppe, J., and Dahlen, F.A., 1983, Mechanics of fold-and-thrust belts and accretionary wedges: *Journal of Geophysical Research*, v. 88, p. 1153–1172, doi: 10.1029/JB088iB02p01153.

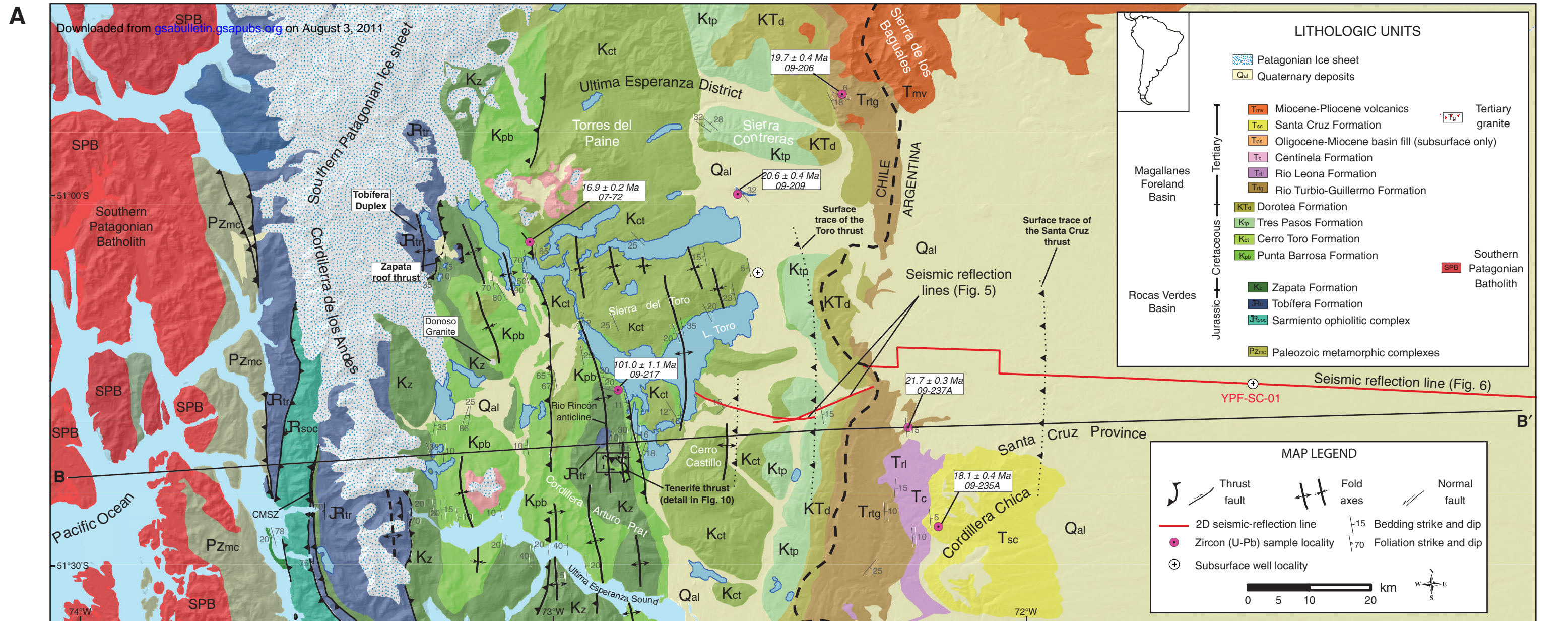
- DeCelles, P.G., 2004, Late Jurassic to Eocene evolution of the Cordilleran thrust belt and foreland basin system, western USA: *American Journal of Science*, v. 304, p. 105–168, doi: 10.2475/ajs.304.2.105.
- DeCelles, P.G., and DeCelles, P.C., 2001, Rates of shortening, propagation, underthrusting, and flexural wave migration in continental orogenic systems: *Geology*, v. 29, no. 2, p. 135–138, doi: 10.1130/0091-7613(2001)029<0135:ROSPUA>2.0.CO;2.
- DeCelles, P.G., and Giles, K.A., 1996, Foreland basin systems: *Basin Research*, v. 8, p. 105–123, doi: 10.1046/j.1365-2117.1996.01491.x.
- DeCelles, P.G., and Mitra, G., 1995, History of the Sevier orogenic wedge in terms of critical taper models, northeast Utah and southwest Wyoming: *Geological Society of America Bulletin*, v. 107, p. 454–462, doi: 10.1130/0016-7606(1995)107<0454:HOTSOW>2.3.CO;2.
- Desegaulx, P., Kooi, H., and Cloetingh, S., 1991, Consequences of foreland basin development on thinned continental lithosphere: Application to the Aquitaine basin (SW France): *Earth and Planetary Science Letters*, v. 106, p. 116–132, doi: 10.1016/0012-821X(91)90067-R.
- Dewey, J.F., and Bird, J.M., 1970, Mountain belts and the new global tectonics: *Journal of Geophysical Research*, v. 75, p. 2625–2647, doi: 10.1029/JB075i014p02625.
- De Wit, M.J., and Stern, C.R., 1981, Variations in the degree of crustal extension during formation of a back-arc basin: *Tectonophysics*, v. 72, p. 229–260, doi: 10.1016/0040-1951(81)90240-7.
- Dickinson, W.R., 1976, Plate Tectonic Evolution of Sedimentary Basins: *American Association of Petroleum Geologists (AAPG) Continuing Education Course Notes Series 1*, 62 p.
- Dickinson, W.R., and Snyder, W.S., 1978, Plate tectonics of the Laramide orogeny, in Matthews, V., ed., *Laramide Folding Associated with Basement Block Faulting in the Western United States*: *Geological Society of America Memoir 151*, p. 355–366.
- Dott, R.H., Jr., Winn, R.D., Jr., DeWit, M.J., and Bruhn, R.L., 1977, Tectonic and sedimentary significance of Cretaceous Tekeka Beds of Tierra del Fuego: *Nature*, v. 266, p. 620–622, doi: 10.1038/266620a0.
- ENAP, 1978, Mapa geológico de la XII Region, Magallanes y Antártica Chilena, Chile: Santiago, Empresa Nacional del Petróleo Depto. de Exploraciones, scale 1:500,000.
- Fildani, A., and Hessler, A.M., 2005, Stratigraphic record across a retroarc basin inversion: Rocas Verdes–Magallanes Basin, Patagonian Andes: *Geological Society of America Bulletin*, v. 117, p. 1596–1614, doi: 10.1130/B25708.1.
- Fildani, A., Cope, T.D., Graham, S.A., and Wooden, J.L., 2003, Initiation of the Magallanes foreland basin: Timing of the southernmost Patagonian Andes orogeny revised by detrital zircon provenance analysis: *Geology*, v. 31, p. 1081–1084, doi: 10.1130/G20016.1.
- Fildani, A., Romans, B.W., Fosdick, J.C., Crane, W.H., and Hubbard, S.M., 2008, Orogenesis of the Patagonian Andes as reflected by basin evolution in southernmost South America: *Arizona Geological Society Digest*, v. 22, p. 259–268.
- Fildani, A., Hubbard, S.M., and Romans, B.W., 2009, Stratigraphic Evolution of Deep-Water Architecture: Examples of Controls and Depositional Styles from the Magallanes Basin, Southern Chile: *Society for Sedimentary Geology Field Trip Guidebook*, v. 10, 73 p.
- Flemings, P.B., and Jordan, T.E., 1990, Stratigraphic modeling of foreland basins: Interpreting thrust deformation and lithosphere rheology: *Geology*, v. 18, p. 430–434, doi: 10.1130/0091-7613(1990)018<0430:SMOFBI>2.3.CO;2.
- Forsythe, R.D., 1982, The late Paleozoic to early Mesozoic evolution of southern South America: A plate tectonic interpretation: *Journal of the Geological Society of London*, v. 139, p. 671–682, doi: 10.1144/gsjgs.139.6.0671.
- Forsythe, R.D., and Mpodozis, C., 1979, El archipiélago Madre de Dios, Patagonia Occidental, Magallanes: Rasgos generales de la estratigrafía y estructura del basamento pre-Jurásico Superior: *Revista Geológica de Chile*, v. 7, p. 13–29.
- Fosdick, J.C., 2008, Assessing deformation and exhumation patterns in the Magallanes foreland basin and Andean fold-and-thrust belt: A progress report: *Stanford Project on Deep-Water Depositional Systems (SPODDS) Proceedings*, v. 16, p. 103–131.
- Galaz, G., Hervé, F., and Calderón, M., 2005, Metamorfismo y deformación de la Formación Tobifera en la cordillera Riesco, región de Magallanes Chile: Evidencias para su evolución tectónica: *Revista de la Asociación Geológica Argentina*, v. 60, no. 4, p. 1–18.
- Galeazzi, J.S., 1998, Structural and stratigraphic evolution of the western Malvinas Basin, Argentina: *American Association of Petroleum Geologists Bulletin*, v. 82, p. 596–636.
- García-Castellanos, D., 2002, Interplay between lithospheric flexure and river transport in foreland basins: *Basin Research*, v. 14, p. 89–104, doi: 10.1046/j.1365-2117.2002.00174.x.
- Ghiglione, M.C., and Cristallini, E.O., 2007, Have the southernmost Andes been curved since Late Cretaceous time? An analog test for the Patagonian orocline: *Geology*, v. 35, p. 13–16, doi: 10.1130/G22770A.1.
- Ghiglione, M.C., and Ramos, V.A., 2005, Progression of deformation and sedimentation in the southernmost Andes: *Tectonophysics*, v. 405, p. 25–46, doi: 10.1016/j.tecto.2005.05.004.
- Goring, M.L., Kay, S.M., Zeitler, P.K., Ramos, V.A., Rubiolo, D., Fernandez, M.I., and Panza, J.L., 1997, Neogene Patagonian plateau lavas: Continental magmas associated with ridge collision at the Chile triple junction: *Tectonics*, v. 16, p. 1–17, doi: 10.1029/96TC03368.
- Graham, S.A., Hendrix, M.S., Wang, L.B., and Carroll, A.R., 1993, Collisional successor basins of western China: impact of tectonic inheritance on sand composition: *Geological Society of America Bulletin*, v. 105, p. 323–344, doi: 10.1130/0016-7606(1993)105<0323:CSBOWC>2.3.CO;2.
- Guillaume, B., Martinod, J., Husson, L., Roddaz, M., and Riquielme, R., 2009, Neogene uplift of central eastern Patagonia: Dynamic response to active spreading ridge subduction?: *Tectonics*, v. 28, doi: 10.1029/2008TC002324.
- Harambour, S.M., 2002, Deep-seated thrusts in the frontal part of the Magallanes fold and thrust belt, Ultima Esperanza, Chile, in *15th Congreso Geológico Argentino: Actas*, v. 3, p. 232.
- Hervé, F., Fanning, C.M., and Pankhurst, R.J., 2003, Detrital zircon age patterns and provenance of the metamorphic complexes of southern Chile: *Journal of South American Earth Sciences*, v. 16, p. 107–123.
- Hervé, F., Godoy, E., Mpodozis, C., and Fanning, M., 2004, Monitoring magmatism of the Patagonian Batholith through the U-SHRIMP dating of detrital zircons in sedimentary units of the Magallanes Basin: *Bolletino dei Geofisica Teorica ed Applicata*, v. 45, p. 113–117.
- Hervé, F., Massonne, H.-J., Calderón, M., and Theye, T., 2007a, Metamorphic *P-T* conditions of Late Jurassic rhyolites in the Magallanes fold and thrust belt, Patagonian Andes, Chile: *Journal of Iberian Geology*, v. 33, p. 5–16.
- Hervé, F., Pankhurst, R.J., Fanning, C.M., Calderón, M., and Yaxley, G.M., 2007b, The South Patagonian Batholith: 150 my of granite magmatism on a plate margin: *Lithos*, v. 97, p. 373–394, doi: 10.1016/j.lithos.2007.01.007.
- Hilley, G.E., Blisniuk, P.M., and Strecker, M.R., 2005, Mechanics and erosion of basement-cored uplift provinces: *Journal of Geophysical Research*, v. 110, doi: 10.1029/2005JB003704.
- Hubbard, S.M., Romans, B.W., and Graham, S.A., 2008, Deep-water foreland basin deposits of the Cerro Toro Formation, Magallanes Basin, Chile: Architectural elements of a sinuous basin axial channel belt: *Sedimentology*, v. 55, p. 1333–1359, doi: 10.1111/j.1365-3091.2007.00948.x.
- Hubbard, S.M., Fildani, A., Romans, B.W., Covault, J.A., and McHargue, T.R., 2010, High-relief slope clinoform development: Insights from outcrop, Magallanes Basin, Chile: *Journal of Sedimentary Research*, v. 80, p. 357–375, doi: 10.2110/jsr.2010.042.
- Ingle, J.C., Jr., 1992, Subsidence of the Japan Sea: Stratigraphic evidence from the ODP sites and onshore sec-
- tions, in Tamaki, K., et al., *Proceedings of the Ocean Drilling Program, Scientific Results, Legs 127/128: College Station, Texas, Ocean Drilling Program*, p. 1197–1218.
- Jordan, T.E., 1981, Thrust loading and foreland basin evolution, Cretaceous, western United States: *American Association of Petroleum Geologists Bulletin*, v. 65, p. 2506–2520.
- Jordan, T.E., and Allmendinger, R.W., 1986, The Sierras Pampeanas of Argentina: A modern analogue of Rocky Mountain foreland deformation: *American Journal of Science*, v. 286, p. 737–764, doi: 10.2475/ajs.286.10.737.
- Katz, H.R., 1963, Revision of Cretaceous stratigraphy in Patagonian cordillera of Ultima Esperanza, Magallanes Province, Chile: *American Association of Petroleum Geologists Bulletin*, v. 47, p. 506–524.
- Keen, C.E., and de Voogd, B., 1988, The continent-ocean boundary at the rifted margin off eastern Canada: New results from deep seismic reflection studies: *Tectonics*, v. 7, p. 107–124, doi: 10.1029/TC007i01p0107.
- Klepeis, K.A., 1994, Relationship between uplift of the metamorphic core of the southernmost Andes and shortening in the Magallanes foreland fold and thrust belt, Tierra del Fuego, Chile: *Tectonics*, v. 13, p. 882–904, doi: 10.1029/94TC00628.
- Klepeis, K.A., and Austin, J.A., Jr., 1997, Contrasting styles of superimposed deformation in the southernmost Andes: *Tectonics*, v. 16, p. 755–776, doi: 10.1029/97TC01611.
- Klepeis, K.A., Betka, P., Clarke, G., Fanning, M., Hervé, F., Rohas, L., Mpodozis, C., and Thomson, S., 2010, Continental underthrusting and obduction during the Cretaceous closure of the Rocas Verdes rift basin, Cordillera Darwin, Patagonian Andes: *Tectonics*, v. 29, doi: 10.1029/2009TC002610.
- Kraemer, P.E., 1998, Structure of the Patagonian Andes: Regional balanced cross section at 50°S, Argentina: *International Geology Review*, v. 40, p. 896–915, doi: 10.1080/00206819809465244.
- Kraemer, P.E., 2003, Orogenic shortening and the origin of the Patagonian orocline (56°S Lat): *Journal of South American Earth Sciences*, v. 15, p. 731–748, doi: 10.1016/S0895-9811(02)00132-3.
- Lawrence, J.F., and Wiens, D.A., 2004, Combined receiver-function and surface wave phase-velocity inversion using a Niching genetic algorithm: Application to Patagonia: *Bulletin of the Seismological Society of America*, v. 94, p. 977–987, doi: 10.1785/0120030172.
- Lisle, R.J., 1992, Constant bed-length folding: Three-dimensional geometrical implications: *Journal of Structural Geology*, v. 14, p. 245–252, doi: 10.1016/0191-8141(92)90061-Z.
- Lonsdale, P., 1995, Segmentation and disruption of the East Pacific Rise in the mouth of the Gulf of California: *Marine Geophysical Researches*, v. 17, p. 323–359, doi: 10.1007/BF01227039.
- Lowell, J.D., 1995, Mechanics of basin inversion from worldwide examples, in Buchanan, J.G., and Buchanan, P.G., eds., *Basin Inversion: Geological Society of America Special Paper 88*, p. 39–57.
- Ludwig, K.R., 2000, *SQUID 1.00: A User's Manual: Berkeley Geochronology Center Special Publication 2*, 77 p.
- Macellari, C.E., Barrio, C.A., and Manassero, M.J., 1989, Upper Cretaceous to Paleocene depositional sequences and sandstone petrography of south-western Patagonia (Argentina and Chile): *Journal of South American Earth Sciences*, v. 2, p. 223–239, doi: 10.1016/0895-9811(89)90031-X.
- Malumíán, N., and Caramés, A., 1997, Upper Campanian–Paleogene from the Rio Turbio coal measures in southern Argentina: Micropaleontology and the Paleocene/Eocene boundary: *Journal of South American Earth Sciences*, v. 10, p. 189–201, doi: 10.1016/S0895-9811(97)00015-1.
- Malumíán, N., Ardolino, A.A., Franchi, M., Remesal, M., and Salan, F., 1999, La sedimentación y el volcanismo terciarios en la Patagonia extraandina, in Caminos, R., eds., *Geología Argentina: Instituto de Geología y Recursos Naturales, Servicio Geológico Minero Argentino, Anales*, v. 29, p. 557–612.
- Malumíán, N., Panza, J.L., Parisi, C., Nañez, C., Caramés, A., and Torre, A., 2001, Hoja Geológica 5172-III,

- Yacimiento Río Turbio: Servicio Geológico Minero Argentino, Boletín, v. 247, 180 p., scale 1:250,000.
- Marsaglia, K.M., 1995, Intercar and backarc basins, in Busby, C., and Ingersoll, R.V., eds., *Tectonics of Sedimentary Basins*: Cambridge, Massachusetts, Blackwell, p. 299–329.
- Matenco, L., Bertottio, G., Cloetingh, and Dinu, C., 2003, Subsidence analysis and tectonic evolution of the external Carpathian-Moesian platform during Tertiary times: *Sedimentary Geology*, v. 156, p. 71–94.
- McKenzie, D., and Bickle, M.J., 1988, The volume and composition of melt generated by extension of the lithosphere: *Journal of Petrology*, v. 29, p. 625–679.
- Michael, P.J., 1983, Emplacement and Differentiation of Miocene Plutons in the Foothills of the Southernmost Andes [Ph.D. thesis]: New York, Columbia University, 367 p.
- Michel, J., Baumgartner, L., Putlitz, B., Schaltegger, U., and Ovtcharova, M., 2008, Incremental growth of the Patagonian Torres del Paine laccolith over 90 k.y.: *Geology*, v. 36, p. 459–462.
- Natland, M.L., Gonzalez, P.E., Canon, A., and Ernst, M., 1974, A System of Stages for Correlation of Magallanes Basin Sediments: *Geological Society of America Memoir* 139, 126 p.
- Olivero, E.B., and Malumián, N., 2008, Mesozoic–Cenozoic stratigraphy of the Fuegian Andes, Argentina: *Geologica Acta*, v. 6, p. 5–18, doi: 10.1344/105.000000238.
- Pankhurst, R.J., Riley, T.R., Fanning, C.M., and Kelley, S.P., 2000, Episodic silicic volcanism in Patagonia and Antarctic Peninsula: Chronology of magmatism associated with the break-up of Gondwana: *Journal of Petrology*, v. 41, p. 605–625, doi: 10.1093/petrology/41.5.605.
- Pankhurst, R.J., Rapela, C.W., Loske, W.P., Fanning, C.M., and Márquez, M., 2003, Chronological study of the pre-Permian basement rocks of southern Patagonia: *Journal of South American Earth Sciences*, v. 16, p. 27–44, doi: 10.1016/S0895-9811(03)00017-8.
- Parras, A., Griffin, M., Feldmann, R., Casadio, S., Schweitzer, C., and Marensi, S., 2008, Correlation of marine beds based on Sr- and Ar-date determinations and faunal affinities across the Paleogene/Neogene boundary in southern Patagonia, Argentina: *Journal of South American Earth Sciences*, v. 26, p. 204–216, doi: 10.1016/j.jsames.2008.03.006.
- Pearce, J.A., 2003, Supra-subduction zone ophiolites: The search for modern analogues, in Dilek, Y., and Newcomb, S., eds., *Ophiolite Concept and the Evolution of Geological Thought*: Geological Society of America Special Paper 373, p. 269–293.
- Polonia, A., Torelli, L., Brancolini, G., and Loreto, M.-F., 2007, Tectonic accretion versus erosion along the southern Chile Trench: Oblique subduction and margin segmentation: *Tectonics*, v. 26, doi: 10.1029/2006TC001983.
- Rabinowitz, P.D., and La Brecque, J., 1979, The Mesozoic South Atlantic Ocean and evolution of its continental margin: *Journal of Geophysical Research*, v. 84, p. 5973–6002, doi: 10.1029/JB084iB11p05973.
- Ramos, V.A., 1989, Andean Foothills structures in northern Magallanes Basin, Argentina: *American Association of Petroleum Geologists Bulletin*, v. 73, p. 887–903.
- Ramos, V.A., 2005, Seismic ridge subduction and topography: Foreland deformation in the Patagonian Andes: *Tectonophysics*, v. 399, p. 73–86, doi: 10.1016/j.tecto.2004.12.016.
- Ramos, V.A., and Kay, S.M., 1992, Southern Patagonian plateau basalts and deformation: Backarc testimony of ridge collisions: *Tectonophysics*, v. 205, p. 261–282, doi: 10.1016/0040-1951(92)90430-E.
- Ramos, V.A., Cristallini, E.O., and Pérez, D.J., 2002, The Pampean flat-slab of the Central Andes: *Journal of South American Earth Sciences*, v. 15, p. 59–78, doi: 10.1016/S0895-9811(02)00006-8.
- Rapalini, A.E., Calderón, M., Singer, S., Hervé, F., and Cordani, U., 2008, Tectonic implications of a paleomagnetic study of the Sarmiento ophiolitic complex, southern Chile: *Tectonophysics*, v. 452, p. 29–41, doi: 10.1016/j.tecto.2008.01.005.
- Riccardi, A.C., and Rolleri, E.O., 1980, Cordillera Patagónica Austral: Actas Segundo Simposio de Geología Regional Argentina, v. 2, p. 1173–1306.
- Robertson, M.S., Wiens, D.A., Koper, K.D., and Vera, E., 2003, Crustal and upper mantle structure of southernmost South America inferred from regional waveform inversion: *Journal of Geophysical Research*, v. 108, p. 2038, doi: 10.1029/2002JB001828.
- Rojas, L., and Mpodozis, C., 2006, Geología Estructural de la Faja Plegada y Corrida del Sector Chileno de Tierra del Fuego, Andes Patagónicos Australes: Antofagasta, Chile, XI Congreso Geológico Chileno Proceedings, v. 11, p. 325–328.
- Romans, B.W., Hubbard, S.M., and Graham, S.A., 2009a, Stratigraphic evolution of an outcropping continental slope system, Tres Pasos Formation at Cerro Divisadero, Chile: Insights into slope processes and evolution: *Sedimentology*, v. 56, p. 737–764, doi: 10.1111/j.1365-3091.2008.00995.x.
- Romans, B.W., Fildani, A., Graham, S.A., Hubbard, S.M., and Covault, J.A., 2009b, Importance of predecessor basin history on sedimentary fill of a retroarc foreland basin: Provenance analysis of the Cretaceous Magallanes basin, Chile (50°52'S): *Basin Research*, v. 22, doi: 10.1111/j.1365-2117.2009.00443.x.
- Romans, B.W., Fildani, A., Hubbard, S.M., Covault, J.A., Fosdick, J.C., and Graham, S.A., 2011, Evolution of deep-water stratigraphic architecture, Magallanes Basin, Chile: *Marine and Petroleum Geology*, v. 28, p. 612–628, doi: 10.1016/j.marpetgeo.2010.05.002.
- Royden, L.H., and Karner, G.D., 1984, Flexure of lithosphere beneath Apennine and Carpathian foredeep basins: evidence for an insufficient topographic load: *American Association of Petroleum Geologists Bulletin*, v. 68, p. 704–714.
- Sánchez, A., 2006, Proveniencia Sedimentaria de los Estratos de Cabo Nariz y Formación Cerro Toro, Cretácico Tardío-Paleoceno, Magallanes, Chile [M.Sc. dissertation]: Santiago, Universidad de Chile, 153 p.
- Sánchez, A., Hervé, F., and Saint-Blanquat, M., 2008, Relations between plutonism in the back-arc region in southern Patagonia and Chile Rise subduction: A geochronological review: *International Symposium on Andean Geodynamics Proceedings*: Paris, Université de Nice Sophia Antipolis, p. 485–488.
- Sanders, C.A.E., Andriessen, P.A.M., and Cloetingh, S.A.P.L., 1999, Life cycle of the East Carpathian orogens: Erosion history of a doubly vergent critical wedge assessed by fission track thermochronology: *Journal of Geophysical Research*, v. 104, p. 29,095–29,112, doi: 10.1029/1998JB900046.
- Scott, K.M., 1966, Sedimentology and dispersal patterns of a Cretaceous flysch sequence, Patagonian Andes, southern Chile: *American Association of Petroleum Geologists Bulletin*, v. 50, p. 72–107.
- Soffia, C., José, M., Harambour, P., and Salvador, S., 1988, Estructuras en el cinturón plegado y fallado de Última Esperanza, Magallanes, Chile: Departamento de Geología, Facultad de Ciencias Físicas y Matemáticas, Universidad de Chile, Comunicaciones Serie 22, v. 39, p. 36.
- Stern, C.R., 1980, Geochemistry of Chilean ophiolites: Evidence of the compositional evolution of the mantle source of back-arc basin basalts: *Journal of Geophysical Research*, v. 85, p. 955–966, doi: 10.1029/JB085iB02p00955.
- Stern, C.R., and de Wit, M.J., 2003, Rocas Verdes ophiolites, southernmost South America: Remnants of progressive stages of development on oceanic-type crust in a continental margin back-arc basin, in Dilek, Y., and Robinson, P.T., eds., *Ophiolites in Earth History*: Geological Society of London Special Publication 218, p. 665–683.
- Stewart, J., Cruzat, A., Page, B., Suárez, M., and Stambuk, V., 1971, Estudio Geológico Económico de la Cordillera Patagónica entre los Paralelos 51°00' y 53°30' Lat. S, Provincia de Magallanes: Santiago, Chile, Instituto de Investigaciones Geológicas (Inédito), 174 p.
- Suárez, M., 1979, A late Mesozoic island arc in the southern Andes, Chile: *Geological Magazine*, v. 116, p. 181–190.
- Suárez, M., and Pettigrew, T.H., 1976, An Upper Mesozoic island-arc-back-arc system in the southern Andes and south Georgia: *Geological Magazine*, v. 113, p. 305–328, doi: 10.1017/S0016756800047592.
- Suárez, M., de la Cruz, R., and Bell, C.M., 2000, Timing and origin of deformation along the Patagonian fold and thrust belt: *Geological Magazine*, v. 137, p. 345–353, doi: 10.1017/S0016756800004192.
- Suppe, J., 1983, Geometry and kinematics of fault-bend folding: *American Journal of Science*, v. 283, p. 684–721, doi: 10.2475/ajs.283.7.684.
- Tamaki, K., and Honza, E., 1991, Global tectonics and formation of marginal basins: Role of the western Pacific: *Episodes*, v. 14, p. 224–230.
- Tanner, P.W.G., 1989, The flexural-slip mechanism: *Journal of Structural Geology*, v. 11, p. 635–655, doi: 10.1016/0191-8141(89)90001-1.
- Thomson, S.N., Hervé, F., and Stockhert, B., 2001, The Mesozoic–Cenozoic denudation history of the Patagonian Andes (southern Chile) and its correlation to different subduction processes: *Tectonics*, v. 20, p. 693–711, doi: 10.1029/2001TC900013.
- Tower, D.B., 1980, Geological evaluation, Western Magallanes Basin, Southern Chile: Santiago, Chile, Archico Tecnico, Empresa Nacional del Petróleo (Magallanes), 15 p.
- Watts, A.B., 1992, The effective elastic thickness of the lithosphere and the evolution of foreland basins: *Basin Research*, v. 4, p. 169–178, doi: 10.1111/j.1365-2117.1992.tb00043.x.
- Willett, S., Beaumont, C., and Fullsack, P., 1993, Mechanical model for the tectonics of doubly vergent compressional orogens: *Geology*, v. 21, p. 371–374, doi: 10.1130/0091-7613(1993)021<0371:MMFTTO>2.3.CO;2.
- Wilson, T.J., 1983, Stratigraphic and Structural Evolution of the Ultima Esperanza Foreland Fold-and-Thrust Belt, Patagonian Andes, Southern Chile [Ph.D. thesis]: New York, Columbia University, 360 p.
- Wilson, T.J., 1991, Transition from back-arc to foreland basin development in southernmost Andes: Stratigraphic record from the Ultima Esperanza District, Chile: *Geological Society of America Bulletin*, v. 103, p. 98–111, doi: 10.1130/0016-7606(1991)103<0098:TFBATF>2.3.CO;2.
- Winn, R.D., Jr., and Dott, R.H., Jr., 1979, Deep-water fan-channel conglomerates of Late Cretaceous age, southern Chile: *Sedimentology*, v. 26, p. 203–228, doi: 10.1111/j.1365-3091.1979.tb00351.x.
- Winslow, M.A., 1982, The structural evolution of the Magallanes Basin and neotectonics in the southernmost Andes: *Bulletin of the International Union of Geological Sciences*, v. 4, p. 143–154.

SCIENCE EDITOR: N. RIGGS  
ASSOCIATE EDITOR: R.W.H. BUTLER

MANUSCRIPT RECEIVED 5 JANUARY 2010  
REVISED MANUSCRIPT RECEIVED 29 JULY 2010  
MANUSCRIPT ACCEPTED 13 NOVEMBER 2010

Printed in the USA



**B**

Kinematic evolution of the Patagonian retroarc fold-and-thrust belt and Magallanes foreland basin, Chile and Argentina, 51°30'S

Fosdick et al.

Figure 3.

Supplement to: *Geological Society of America Bulletin*, v. 123; no. 9/10; doi: 10.1130/B30242.S1

© Copyright 2011 Geological Society of America

**Figure 3.** (A) Geologic map of the Patagonian fold-and-thrust belt and Magallanes foreland basin between 50°S and 52°S, encompassing the Última Esperanza District in Chile and the Santa Cruz Province in Argentina. Geology is based on new mapping and adaptation of previous mapping by Wilson (1983) and others (Stewart et al., 1971; Allen, 1982; Soffia et al., 1988; Malumíán et al., 2001; Fildani and Hessler, 2005; Calderón et al., 2007a; Romans et al., 2009a). The structural cross section along B-B' is depicted in part B. The locations of two-dimensional (2-D) seismic-reflection lines are shown in red along the eastern margin of the study area. Zircon U/Pb geochronologic sample localities are indicated on the map using magenta circles. (B) Structural cross section B-B' of the Patagonian thrust belt and Magallanes retroforeland basin compiled from geologic mapping and subsurface data. The locations of seismic-reflection data from Figures 5 and 6 are indicated with black boxes. The red dashed line within the Paleozoic basement indicates the zone of inferred regional uplift beneath Patagonia based on structural reconstructions presented in this paper (Fig. 10). SPB—Southern Patagonian Batholith; RVB—Rocas Verdes Basin.